

# THE ANALYSIS OF SHUTTLE-TANKER AND FLOATING STORAGE OFFLOADING DURING BERTHING OPERATIONS AT OFFSHORE NIGERIA, IN RESPONSE TO SOLITON AND SQUALL EVENTS



International Chair in Mathematical Physics and Applications.  
(ICMPA-UNESCO Chair)

Master of Science in Physical Oceanography and Applications.

Presented by:

**GHOMSI KONGA Serge**

Faculty of Science and Technology (FAST)  
University of Abomey-Calavi (UAC)  
Cotonou, Republic of Benin





**University of Abomey-Calavi (UAC), BENIN  
Faculty of Science and Technology (FAST)  
International Chair in Mathematical Physics and  
Applications  
(ICMPA-UNESCO Chair )**

*M.Sc N°...../M.Sc/ICMPA/FAST/UAC/2015.*

**THE ANALYSIS OF SHUTTLE-TANKER AND FLOATING  
STORAGE OFFLOADING DURING BERTHING  
OPERATIONS AT OFFSHORE NIGERIA, IN RESPONSE  
TO SOLITON AND SQUALL EVENTS**

Master Thesis of Science  
In  
Physical Oceanography and Applications  
Presented by:

**GHOMSI KONGA Serge**

**Supervisors:**

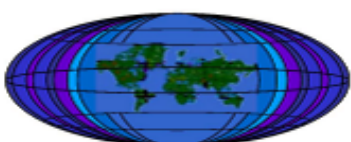
Michael QUINNELL, Fugro GEOS, Wallingford, UK.  
Dr Veronique COCHIN, Fugro GEOS, Wallingford, UK.

**Jury:**

**President:** Pr Nicholas Hall, UPS Toulouse III.  
**Examinator:** Dr Regina FOLORUNSHO, NIOMR, Nigeria.  
**Reporter:** Dr Yves DU PENHOAT, ICMPA, IRD/UAC.

Cotonou, Rep. of Benin, October 2015

## **SPONSORS**



**Chaire Internationale en  
Physique Mathématique  
et Applications**



**Université Paul Sabatier /  
chaires croisées**



Institut de recherche  
pour le développement

**Programme chaires  
croisées (Formation et  
Recherche en  
océanographie Physique  
et Applications en  
Afrique de l'ouest)**



**Société Total / Total  
professeurs associés**



**Fugro GEOS  
(Global Environmental  
and Ocean Sciences)**

---

---

## Dedication

---

To the husband of my sister Nathalie,

Who died during the writing of this report

Deumaga, Hugues

---

# Acknowledgement

---

First, I would like to thank Fugro GEOS Ltd company for proposing this topic and particularly the Managing Director, Anthony Gaffney, for his support during project. I address my special thanks to my supervisors, Michael Quinnell (Fugro GEOS, UK) and Dr Veronique Cochon (Fugro GEOS, UK) for their availability and for helping to familiarize me to oceanography applied to offshore industry. I also thank Marwa El-Sawify and Jane Crawford, both of Fugro GEOS in Wallingford, United Kingdom for their help in administrative procedure. I can't forget to thank Elaine Dickins and Jill Bradon from Fugro GEOS Consultancy and Alex Webb from Fugro GEOS Offshore division for their input on the soliton detection.

Also worthy of acknowledgement is TOTAL Ltd. for their support.

I address special thanks to Dr Gael Alory and Dr Yves Du Penhoat for their invaluable support during this training.

I thank the jury members of this thesis, particularly Dr Regina Folorunsho who agreed to inspect this report.

I would like to thank Professor Norbert Hounkounou (President and holder of ICMPA/UAC), Pr Nick Hall, Pr Ezinvi Baloïtcha (Scientific Secretary), Dr Raphael Almar, Dr Isabel Dadou, Dr P. Van Beek, Dr Alexei V. Kouarev, Dr Juliette Mignot, Dr Angelique Melet, Mme Claire Channeliere, Jean M. Dumay, Dr Ousmane Dine, Dr Dominique Dargone, Dr Thierry Delcroix and Mr François Adjibode for their contribution to my training. I also address special thanks to Amos Wirngo, Mesmin Awo, Gregoire Abessolo and Guy H. Houngue for their support, to Dr Serge E. Mkam and Dr Roger Keumo for his advice.

I will never forget contributions of my classmates: Armand Bahini and Nouhoum Biaou (Benin), Sakaros Bogning and Justine Yandjimain (Cameroon), Etienne Le Vaillant (France), Minto Dimoune and Koubodanna N'janna (Togo), who helped me to improve this work.

Specially, I express my gratitude to my guardian in Cotonou Mireille Djuikouo, for her daily support and love and to my older brother Guy H. Fodju for his financial support.

I also address my thanks, to my parents Colette & Joseph Takou in Yaounde and Marie & Bernard Konga in Douala for their moral support and advice, to my uncle Dr Mkounga Pierre for his academic advice, to Boukam, Nouayou and Homsi families for their affection, to my brothers Mathurin Soh, Dr Cécile Kouam, Fridolin Melong, Dr Elise Pouemi, Raoul Kamga, Samuel Ghomsi and my sister Nathalie Mamgue for their daily love.

Finally, I would like to thank my friends Dr Sama Arjika, Giresse Nameni, Myriam Tapi, Narcisse Mpagang, Osée Fokoua, Peguy Nouemsi, Blanche Djeufack, Willy Motin, Adjany Tatchou and Stella Nkwinkwa, for their encouragement.

# List of Acronyms and Abbreviations

---

<b>ADCP</b>	Acoustic Doppler Current Profiler
<b>API</b>	American Petroleum Institute
<b>CALM</b>	Catenary Anchor Leg Monitoring
<b>ERTS</b>	Earth Resource Technology Satellite
<b>FPSO</b>	Floating Production Storage Offloading
<b>FSO</b>	Floating Storage Offloading
<b>GEOS</b>	Global Environmental and Ocean Sciences
<b>GOG</b>	Gulf Of Guinea
<b>GPS</b>	Global Position System
<b>HW</b>	Higher Water
<b>ITCZ</b>	Inter-Tropical Convergence Zone
<b>ISO</b>	International Standards Organisation
<b>ISW</b>	Internal Solitary Wave
<b>KDV</b>	Korteweg De Vrie
<b>LW</b>	Lower Water
<b>OWA</b>	Offshore West Africa
<b>RTK</b>	Real Time Kinematic
<b>SAL</b>	Saharan Air Layer
<b>SAR</b>	Synthetic Aperture Radar
<b>SPM</b>	Single Point Mooring
<b>UK</b>	United Kingdom
<b>UTC</b>	Coordinated Universal Time
<b>USA</b>	United States of America
<b>WAG</b>	West African Gust
<b>WAM</b>	West African Monsoon
<b>WMO</b>	World Meteorological Organization

---

# Abstract

---

Metocean phenomena such as internal solitary waves (ISWs) or solitons , strong highly variable ocean currents and squall can seriously disrupt offshore exploration, development and offloading operations. Statistical analysis of data taken on a oil platform and on a floating storage offloading (FSO), Offshore Nigeria from 12 March 2013 to 27 August 2014, has carried out existence and propagation of solitons and squalls in oil platform field. There are recorded 273 soliton events which likely move from the oil platform to FSO in 1 hour 45 minutes on average, and 95 squall events with a mean rise time of wind speed of 14 minutes. FSO and shuttle tanker responses were studied through analysis of global position system (GPS), heading and mooring hawser tension data. There are founded some periods where the response was violent as on 24 April 2014, where hawser tension increases up to 235 tons. There also are founded an occurrence of tanker's mooring hawsers breaking due to strong soliton event, which occurs on 20 December 2013. Proposals for prediction of these phenomena and violent response of FSO and responses to these events were made.

**Keywords:** **soliton, squall, mooring hawsers, FSO, shuttle tanker, statistical analysis, response.**

---

## Resumé

---

Les phénomènes météorologique et océanographique tels que les ondes solitaires et internes ou solitons, les courants océaniques et les squalls ou lignes de grain peuvent perturber considérablement les phases d'exploration, de développement et d'opération d'un champ pétrolier. Une analyse statistique des données métocéan prises sur une plate forme pétrolière et sur un FSO (*Floating Storage Offloading*), au large du Nigeria du 12 Mars 2013 au 27 Août 2014, a révélé l'existence et la propagation des événements de soliton et de squall dans ce champ pétrolifère. 273 événements de soliton ont été détectés, et se déplaçaient de la plateforme pétrolière au FSO en moyenne de 1 heure 45 minutes. 95 événements de squall ont également été identifiés avec un durée moyenne d'élévation de la vitesse du vent de 14 minutes. Une analyse des réponses du FSO et du Shuttle tanker a été faite à partir des données de position (GPS) du FSO et de tension de la haussière. Un cas de réponse violente du shuttle tanker qui avait eu lieu le 24 Avril 2014 a été analysé avec une tension de la haussière qui a atteint 235 tons. Nous avons aussi identifié un cas de rupture de câble de mouillage de la haussière qui a eu lieu le 20 Décembre 2013 due à un événement extrême de soliton. Quelques propositions ont été faites sur la prévision de ces phénomènes ainsi que des différentes réponses à ces phénomènes.

**Keywords:** **soliton, squall, mouillage, haussière, FSO, shuttle tanker, analyse statistique, réponse.**

---

# List of Figures

---

1.1	<i>Example of rig incident (Goff et al., 2010 [18])</i>	2
1.2	<i>A squall in the strait of Malacca (McPhail, 2014 [27])</i>	3
2.1	<i>Schematic diagram showing the position of the pycnocline (Shanmugam, 2013[34])</i>	4
2.2	<i>A two-layer internal soliton (Jean, 1998[24])</i>	7
2.3	<i>Squall Regions (McPhail, 2014[27])</i>	9
2.4	<i>Squall formation and structure (Fugro GEOS, 2004[16])</i>	9
3.1	<i>Study location, FSO and Oil Platform, Offshore Nigeria [37]</i>	11
3.2	<i>Overview of metocean data acquisition system</i>	13
4.1	<i>24-hour of unfiltered Northward and Eastward velocities, maximum speed and depth integrated speed observed on 23 April 2014, showing two solitons events.</i>	17
4.2	<i>24-hour of Filtered Northward and Eastward velocities, maximum speed and depth integrated speed observed on 23 April 2014, showing two solitons events.</i>	17
4.3	<i>24-hour of Current direction contour, ADCP pitch and roll, Temperature and tidal height observed on 23 April 2014, showing semi-diurnal soliton occurrence.</i>	18
4.4	<i>4-hour of unfiltered Northward and Eastward velocities, maximum speed and depth integrated speed observed on the 23 April 2014, showing one soliton event at 04:45 UTC.</i>	18
4.5	<i>4-hour of Filtered Northward and Eastward velocities, maximum speed and depth integrated speed observed on the 23 April 2014, showing one soliton event at 04:45 UTC.</i>	19
4.6	<i>Current direction, ADCP pitch and roll, Temperature and tidal height plots observed on the 23 April 2014 04:45, showing solitons packet.</i>	19
4.7	<i>Currents speed (top) and direction (bottom) associated with observed soliton.</i>	20
4.8	<i>Current speed, FSO displacement and heading, and hawser tension.</i>	21
4.9	<i>Contour plots of filtered Northward and Eastward velocity.</i>	22
4.10	<i>8-hour contour plots of filtered Northward and Eastward velocity showing a strong soliton event</i>	22
4.11	<i>8-hour plots of current speed and temperature, heading of FSO and Hawser tension, showing the breaking of mooring hawsers due to strong soliton event</i>	23
4.12	<i>Wind speed and direction (a), wind speed gust and direction (b), showing the passage of squall event on 25 March 2014.</i>	24
4.13	<i>Occurrence of squall relative to wind speed (top) and to wind direction (bottom).</i>	25
4.14	<i>Distribution of average monthly squall event over the two years (top) and diurnal distribution in % for 3-hourly intervals (bottom).</i>	26

4.15	<i>20-hour time series plot of FSO rotation and heading showing FSO response during a squall event on 23 February 2014.</i>	27
4.16	<i>Soliton events with tidal range from March 2013 to August 2014.</i>	29
5.1	<i>Contour plots of filtered Northward and Eastward velocity showing the arrival of soliton event at 01:40 on 23 May 2014 at platform.</i>	36
5.2	<i>plots of current speed and temperature (a), FSO displacement and heading (b) and hawser tension (c) showing the response of FSO and mooring hawser to soliton event between 02:45 and 04:00 UTC on 23 May 2014. We can notice an inclination of heading from 240 to 320 °T and an increase of hawser tension up to 78 tons.</i>	36
5.3	<i>Contour plots of filtered Northward and Eastward velocity showing the arrival of 3 soliton events at 16:40 on 8 May 2014, at 03:30 and 12:30 on 9 May 2014 at oil platform</i>	37
5.4	<i>plots of current speed and temperature (a), FSO displacement and heading (b) and hawser tension (c) showing 3 main responses of FSO and mooring hawser to soliton event. We can notice an inclination of heading from 240 to 320 °T and an increase of hawser tension up to 100 tons between 14:00 and 16:45 on 09 May.</i>	37
5.5	<i>Contour plots of filtered Northward and Eastward velocity showing the arrival of 2 soliton events at 00:00 and 13:30 on 31 March 2013 at oil platform</i>	38
5.6	<i>plots of current speed and temperature (a), FSO heading (b) and hawser tension (c) showing 2 main responses of FSO and mooring hawser to soliton event. We can notice an inclination of heading from 300 to 200 °T from 00:45 to 02:10 on 31 March 2013 and an increase of hawser tension up to 120 tons between 14:30 and 15:45 on 31 March 2013.</i>	38
5.7	<i>Contour plots of filtered Northward and Eastward velocity showing the arrival of some soliton events at oil platform</i>	39
5.8	<i>plots of current speed and temperature (a), FSO heading (b) and hawser tension (c) showing FSO and mooring hawser response to soliton event. We can notice an inclination of heading from 240 to 300 °T and increase of hawser tension up to 105 tons between 01:00 and 02:30 on 18 April 2013.</i>	39
5.9	<i>22-hour plots of wind speed and direction (a), FSO displacement and heading (b), showing the response of FSO to arrival of squall event at 17:00. We can notice heading change from 195 to 130 °T and horizontal displacement of FSO.</i>	40
5.10	<i>22-hour plots of wind speed and direction (a), FSO displacement and heading (b), showing the response of FSO to arrival of squall event at 09:30. We can notice heading change from 300 to 10 °T.</i>	40

---

# List of Tables

---

4.1.1 <i>Monthly occurrence of soliton events. MD: Missing Data . . . . .</i>	20
4.2.1 <i>Monthly occurrence of squall events. MD: Missing Data . . . . .</i>	24
4.3.1 <i>Occurrence of Soliton with Tidal Range over the data acquisition period . . . . .</i>	28

---

# Table of Contents

---

<b>Dedication</b>	ii
<b>Acknowledgement</b>	iii
<b>List of Acronyms and Abbreviations</b>	iv
<b>Abstract</b>	v
<b>Resumé</b>	vi
<b>List of Figures</b>	vii
<b>List of Tables</b>	viii
<b>1 Introduction</b>	1
1.1 Presentation of Fugro GEOS . . . . .	1
1.2 Soliton and Squall . . . . .	2
1.2.1 Soliton . . . . .	2
1.2.2 Squall . . . . .	2
1.3 Objectives and Outlines of this Study . . . . .	2
<b>2 Literature Review</b>	4
2.1 Solitons . . . . .	4
2.2 Theoretical Models of Soliton . . . . .	6
2.2.1 Korteweg-de Vries equation . . . . .	6
2.2.2 Energy of Soliton . . . . .	7
2.3 Squall . . . . .	8
2.4 Overview of Shuttle Tanker-FPSO Offloading . . . . .	10
<b>3 Study Area, Data Acquisition and Methodology</b>	11
3.1 Study Area . . . . .	11
3.2 Data Acquisition . . . . .	12
3.2.1 Oil Platform Data . . . . .	12
3.2.2 FSO Data Collected . . . . .	13
3.3 Methodology and Data Analysis . . . . .	13
3.3.1 Data Quality Control . . . . .	14
3.3.2 Soliton identification . . . . .	14
3.3.3 Squall identification . . . . .	14

3.3.4	Analysis of FSO and Tanker Responses . . . . .	15
<b>4</b>	<b>Results and Discussions</b>	<b>16</b>
4.1	Soliton . . . . .	16
4.1.1	Case Analysis . . . . .	16
4.1.2	Solitons Statistics . . . . .	20
4.1.3	FSO and Tanker response during an extreme soliton event . . . . .	21
4.1.4	Analysis of Broken Mooring Hawser Case . . . . .	22
4.2	Squall . . . . .	23
4.2.1	Case analysis . . . . .	23
4.2.2	Squall statistics at FSO . . . . .	24
4.2.3	Annual and Diurnal Variation . . . . .	25
4.2.4	FSO response during an extreme squall event . . . . .	26
4.3	Discussion . . . . .	27
4.3.1	Predictability of soliton events . . . . .	27
4.3.2	Soliton . . . . .	28
4.3.3	Squall . . . . .	28
4.3.4	FSO and Shuttle tanker response . . . . .	29
<b>5</b>	<b>Conclusion and Recommendations</b>	<b>30</b>
5.1	Conclusion . . . . .	30
5.2	Recommendations . . . . .	31
<b>Bibliography</b>		<b>32</b>
<b>Appendix</b>		<b>35</b>
Appendix 1	. . . . .	35
Appendix 2	. . . . .	38

---

CHAPTER 1

---

---

# Introduction

---

Ocean and the Atmosphere are all the time subject to internal and external forcing, which leads to the formation and appearance of natural phenomena such as Squall, Internal Wave and Swell. These phenomena considerably influence the offshore structures or the offloading operations, and can have important consequences for oil companies, including economic losses, human casualties, environmental damages, and loss of credibility by the operating company. Forecasting these phenomena with sufficient time to allow staff to take necessary actions to avoid these negative consequences is an important research area for oil companies. In this context, Fugro GEOS, a service provider on a oil platform in offshore Nigeria has proposed this project to analyse the responses of the FSO and Shuttle Tanker to squall and soliton events during the offshore operations on this FSO.

## 1.1 Presentation of Fugro GEOS

Fugro GEOS is a leading company in the provision of commercial, meteorological and oceanographic (metocean) services and systems in offshore and coastal environment. Fugro GEOS evolved from Wimpey Laboratories, first established in the 1920's, through Wimpol and WEIL to form Fugro Global Environmental and Ocean Sciences (GEOS) in 1994. This was a combined venture with Wimpey more of Fugro Group. In 1996 Fugro GEOS became a wholly-owned subsidiary of the Fugro Group. Fugro GEOS has offices in 11 locations across the globe, it has about 265 employees worldwide and provides services to oil companies, including these operating in African countries (Nigeria, Angola...).

## 1.2 Soliton and Squall

During exploration, development and exploitation phases, the oil companies are exposed to the negative consequences induced by the natural phenomena such as Squall and Soliton.

### 1.2.1 Soliton

Internal solitary waves, commonly known as soliton are large-amplitude and nonlinear internal waves that are associated with strong currents which vary rapidly in time and flow in opposite directions above and below the density interface along which they propagate (Jeans, 1998 [24]). They are generated by the nonlinear deformation of internal tides (Ostrovsky & Stepanyants, 1989 [30]). They are potentially and extremely hazardous to sub-sea oil and gas drilling operations, because of their rapidly varying and sometimes extremely strong associated current velocity and shear. Fraser (1998 [15] & 1999 [14]) has reported one particular incident in the Northern Andaman Sea during the passage of a soliton event, which led the tilt of rig (Fig.1.1) by  $3^\circ$  and an increase in the anchor tension on one side of the rig by almost 25%.

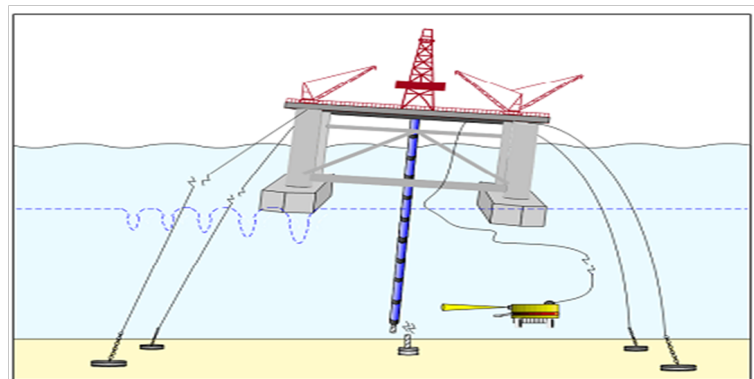


*Fig. 1.1: Example of rig incident (Goff et al., 2010 [18])*

### 1.2.2 Squall

Squalls are mesoscale sudden increases in wind speed that last for a short time. They occur more in the region influenced by ITCZ and are usually associated with severe weather (Fig.1.2). Squalls regularly occur in a squall line associated with harsh thunderstorms. Squalls can influence offshore operations and in many cases drive the design of mooring systems for floating facilities offshore. They are dangerous for connecting tankers to CALMS and FPSOs and can impact berthing operations.

## 1.3 Objectives and Outlines of this Study

Offshore West Africa (OWA) is a region where squalls result in the extreme design loads and offset for the floating systems as the other extreme environmental criteria are relatively mild. OWA is also a region in which many solitons are encountered, due to significant topographic

features which often vary rapidly. Studies of these phenomena are very important for the seismic exploration phase for drilling and offloading operations and for engineering design.

In our case, we study soliton and squall events for offloading operations at a FSO offshore in Nigeria. The passage of these phenomena can disrupt the offloading operation, for example the loading of a shuttle tanker, which can lead to the breaking of the tanker's mooring hawser and significant moving of FSO. Hence, the principal aim of this study is to analyse tanker and FSO response to squall and soliton events during the offloading operation. The specific objectives of this work are to:

- Develop a screening algorithm to identify soliton and squall events on this oil platform and on a FSO, offshore Nigeria;
- Plot the parameters (current speed and direction, ADCP pitch and roll, temperature, wind speed and direction) characterizing these phenomena.
- Quantify characteristics of squall and soliton phenomena encountered in this area (OWA), such as propagation speed and direction, frequency and any correlation with other events (tide for example);
- Study tanker (hawser tension) and FSO (position) response during these events.
- Identify an occurrence of tanker's mooring hawser breaking due to strong soliton event;
- Propose an early warning system based on the prediction a soliton event.

In this report, we discuss the literature review of soliton and squall events in chapter 2. In chapter 3 we present the study area, data acquisition and methods used in this work. Results are presented and discussed by chapter 4. The conclusion and some recommendations are presented in chapter 5.



*Fig. 1.2: A squall in the strait of Malacca (McPhail, 2014 [27])*

# Literature Review

## 2.1 Solitons

Solitary Internal Waves (SIWs) commonly known as solitons, are the large amplitude, non-sinusoidal and non-linear internal waves. They propagate in groups of 2 to 10 isolated waves and are usually associated with rapidly varying and extremely strong current surges (of up to 2m/s in Andaman Sea). They are commonly a feature in the ocean, frequently observed on shallow continental margins as well as in deep water. They are generally associated with depressions of internal density interface as pycnocline (figure 2.1) which may be as large as 100 m and can be extremely steep, with individual solitons typically persisting for between 5 and 30 minutes. The associated currents flow against the direction of propagation in the lower layer resulting in a strong shear across the interface. Pynocline is the primary density stratification layer in ocean.

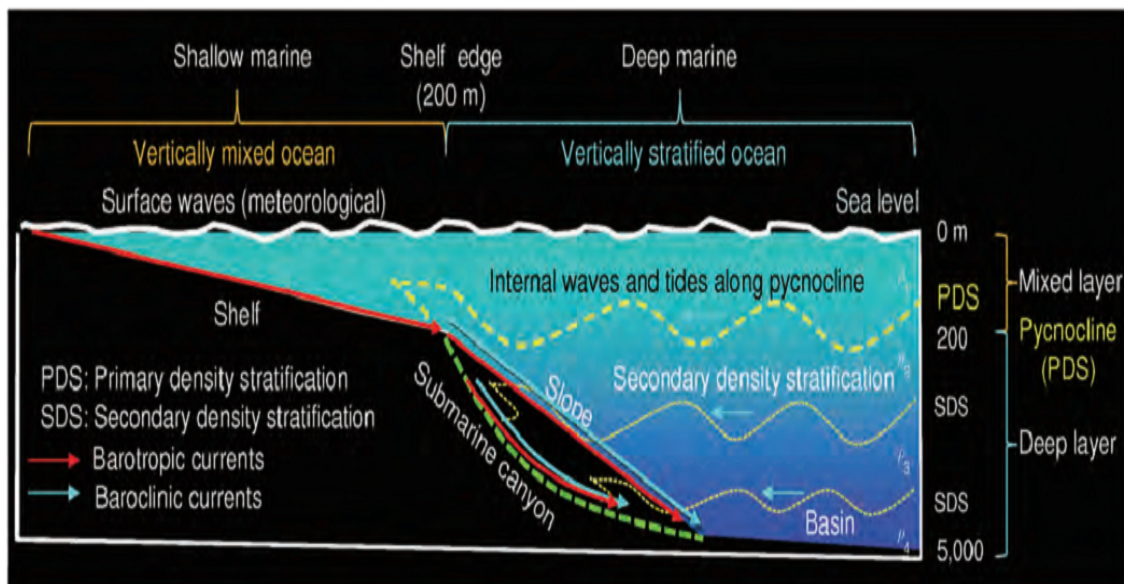


Fig. 2.1: Schematic diagram showing the position of the pycnocline (Shanmugam, 2013[34]).

Conventional theory suggests that solitons are generated when strong tidal currents flow over significant topographic features, such as shelf breaks, sills or sea mounts, in the presence of stratification. They are frequently interpreted as the non-linear manifestations of the internal tide. These waves have complex shape and maintain their coherence, and hence visibility, through non-linear hydrodynamic and as long, quasilinear stripes in imagery (Apel, 1987[3]). The internal wave signatures are made visible by current/wave interactions; wherein the near-surface currents associated with the internal wave locally modulates the surface height spectrum. Primary modulations typically occur at wavelengths ranging between 10 and 50cm to a few meters, but secondary interactions further transport surface wave energy down to sub-centimeter scales. Thus, a roughening of the short-wave portion of the surface wave spectrum takes place in regions of internal wave phase where the currents are convergent.

The earliest recognition of internal solitary waves appears to have been made by John Scott Russell (1808-1882) who reported on the formation of a single, unchanging hump or mound in the shallow water of the Scottish Canal, generated when a towed barge was brought to a sharp halt in the canal. He followed the wave after its passage along the channel without change of form or reduction of speed, for some eight or nine miles on horseback an hour. He observed a gradual reduction of height and lost sight of the wave in the windings of the canal. He called the “*Wave of Translation*”. Russell also demonstrated his observation in an experiment. He used a self-built 30-ft wave tank in his back garden. From this experiment, he observed an empirical relationship between the speed of the wave, its amplitude and the water depth. In 1975, solitons were observed in the New York Bight based on ERTS (Earth Resource Technology Satellite) imagery (Apel et al., 1975[2]). Solitons have also previously been observed in the southern Andaman Sea (with complex bathymetry) by Osborne and Burch in 1980 (Osborne & Burch, 1980 [29]).

George Biddell Airy (in 1845) and Gabriel Stokes (in 1849) found that Russell’s experimental observations conflicted with the existing water wave theories, especially the Isaac Newton’s and Daniel Bernoulli’s theories of hydrodynamics. In 1871, Joseph Valentin Boussinesq established the first mathematical description of waves with permanent form which was still inconsistent with Russell’s observations. In 1895, Diederik Korteweg and Gustav de Vries derived some interesting mathematical properties for a solitary wave. This equation is generally known as KDV (Korteweg De Vrie 2.2.1 ) equation and it was very important for history and comprehension of solitons theory.

The creation of solitons relies on the existence of both intrinsic dispersion and nonlinearity in the medium. The speed of the wave increases depending on the local displacement, the long wave steepens toward a shock-like condition with the consideration of nonlinear effects. In a dispersive system, however, unlike in non-dispersive acoustics, this shock formation is resisted by dispersion. A soliton then represents a balance between these two factors, with a resulting wave of permanent shape which propagates at a speed dependent on its amplitude, the layer depth and the density contrast, among other factors (Apel et al., 2006[5]).

## 2.2 Theoretical Models of Soliton

The first simple first-order “quadratic” nonlinear soliton model was advanced by Korteweg and De Vries in 1897. Since then however additional solitary wave equations have been derived and new solutions found. These equations are based on the equations of hydrodynamics associated to many approximations and depending on the propagation medium of wave.

### 2.2.1 Korteweg-de Vries equation

Let us examine the well-investigated case of a solitary internal wave propagating in an arbitrary stratified but non rotating fluid ( $f = 0$ ). Then let us assume a small dispersion and a small nonlinearity for one-dimensional progressive internal solitary waves propagating in the positive direction of axis  $x$ , the classical Korteweg-de Vries equation can generally be written as:

$$\frac{\partial \eta}{\partial t} + \left(c + \alpha\eta\right) \frac{\partial \eta}{\partial x} + \gamma \frac{\partial^3 \eta}{\partial x^3} = 0 \quad (2.2.1)$$

where  $\eta(x, t)$  is the (normalized) vertical displacement of an isopycnal surface from its equilibrium levels,  $c$ ,  $\alpha$  and  $\gamma$  represent wave phase speed, coefficient of nonlinear effect and coefficient of dispersive effect, respectively. These parameters are defined as:

$$\alpha = \frac{3c\sigma}{2H}, \quad \gamma = \frac{cDH^2}{2} \quad (2.2.2)$$

where  $\sigma$  and  $D$  are non-dimensional parameters describing nonlinearity and high-frequency dispersion, respectively and  $H$  is the water depth.

The well-known solitary solution to Eq.2.2.1 is

$$\eta(x, t) = \eta_0 \operatorname{sech}^2\left(\frac{x - Vt}{L}\right) \quad (2.2.3)$$

where the nonlinear velocity  $V$  and the characteristic width  $L$  of this soliton being related to the linear speed  $c$  and the amplitude of displacement  $\eta_0$  are given by

$$V = c + \frac{\alpha\eta_0}{3}, \quad L^2 = \frac{12\gamma}{\alpha\eta_0}. \quad (2.2.4)$$

The combination of the parameters  $\alpha$  and  $\gamma$  determines the soliton polarity; namely, the sign of  $\eta_0$  is such that  $L^2$  in Eq. 2.2.4 is positive. Thus, if  $\alpha$  is negative, so will be  $\eta_0$ . Therefore the soliton is a wave of isopycnal depression.

Let us consider a two-layer model of an ocean (Fig.2.2), showing amplitude  $\eta_0$ , length scale  $L$ , phase speed  $c$ , zones of surface convergence ( $C$ ) and divergence ( $D$ ). It is continuously stratified with the thicknesses of the upper and lower layer defined as  $h_1$  and  $h_2$  respectively,  $\rho_1$  and  $\rho_2$  are the density of water in upper and lower layer respectively,  $H = h_1 + h_2$  is the water depth,

with

$$\rho(z) = \rho_1 \quad \text{for} \quad 0 > z > -h_1 \quad \text{and} \quad \rho(z) = \rho_2 > \rho_1 \quad \text{for} \quad -h_1 > z > -H.$$

Thus, we have

$$c = \sqrt{\frac{g(\rho_2 - \rho_1)h_1h_2}{\rho_2h_1 + \rho_1h_2}} \simeq \sqrt{\frac{g\delta\rho}{\rho_a} \frac{h_1h_2}{(h_1 + h_2)}} \quad (2.2.5)$$

$$\alpha \simeq \frac{3}{2}c \frac{h_1 - h_2}{h_1h_2} \quad \text{and} \quad \gamma \simeq \frac{ch_1h_2}{6} \quad (2.2.6)$$

$$V = c\left(1 + \frac{\eta_0}{2} \frac{h_1 - h_2}{h_1h_2}\right) \quad \text{and} \quad L^2 = \frac{4(h_1h_2)^2}{3(h_1 - h_2)} \quad (2.2.7)$$

where  $\delta\rho = \rho_2 - \rho_1$  is always small for the ocean and  $\rho_a = 1/2(\rho_1 + \rho_2)$ . The Equations 2.2.6 show that solitons propagate on a thin upper layer over a deeper lower layer are always negative ( $\alpha < 0$ ): depressions, whereas solitons riding on near-bottom layers are elevations.

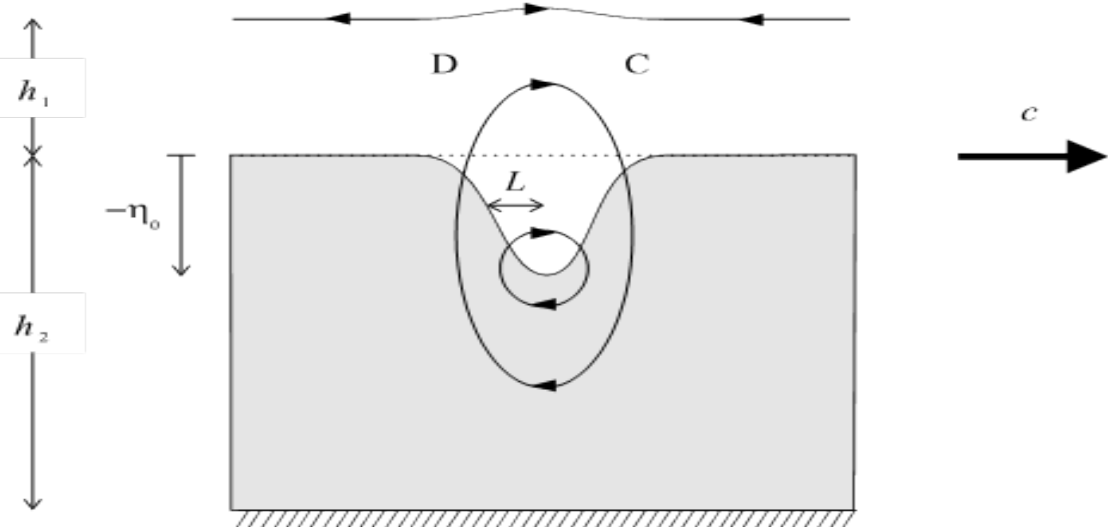


Fig. 2.2: A two-layer internal soliton (Jean, 1998[24]).

## 2.2.2 Energy of Soliton

The energy of an internal solitary wave can be subdivided in both kinetic and potential energies. The potential energy which is the work done against gravitational forces and depend on the vertical position and mass, was defined as

$$E_P = \int_v^{v+dv} \rho g z dv \quad (2.2.8)$$

where  $\rho$ ,  $g$ ,  $z$  and  $v$ ,  $dv$  are the density of water column, the gravity, the vertical displacement of interface, volume, and a volume element respectively.

For a two-layer solitary internal wave, potential energy is:

$$\begin{aligned} E_P &= \int_0^L g \left( \int_{-\eta}^0 \rho_1 z dz + \int_0^\eta \rho_2 z dz \right) dx \\ E_P &= \frac{1}{2} \eta^2 g \delta \rho L \end{aligned} \quad (2.2.9)$$

where  $\delta \rho = \rho_2 - \rho_1$ ,  $L$ ,  $\eta$  are the density difference between two layer, wave length and vertical displacement of interface respectively.

With several assumptions and approximations (for example, that the vertical displacement is far smaller than the vertical length scale (Osborne & Burch, 1980 [29] ) the kinematic energy of a soliton can be written as:

$$\begin{aligned} E_K &= \int_0^L g \left( \int_{-eta}^0 \rho_1 (U_1^2 + W_1^2) dz + \int_0^\eta \rho_2 (U_2^2 + W_2^2) dz \right) dx \\ E_K &= \frac{5}{6} \eta^2 g \delta \rho L \end{aligned} \quad (2.2.10)$$

where  $U_1$ ,  $W_1$  and  $U_2$ ,  $W_2$  are zonal and vertical velocities respectively in the upper layer and in the lower layer. The total energy in this case is:

$$E = \frac{4}{3} \eta^2 g \delta \rho L \quad (2.2.11)$$

## 2.3 Squall

Squalls are convective storms which, near sea level, are characterized by sudden rapid increases in wind speed and sudden shifts in wind direction: a squall event usually lasts less than an hour at a given location. Squalls are also thunderstorms generated on land, which tend to form along lines separating air masses and which usually travel westward (in the tropical area) over the sea. They are a natural phenomenon occurring over a wide range of latitudes and are typically only design events in tropical areas (Fig.2.3).

Squalls form preferentially in regions of atmospheric instability where warm moist air can rise. Latent heat released by condensation of water vapour warms the rising air, making it lighter than the surrounding air and provides the mechanism which drives the squall updraft and formation of Cumulus. The drag of falling precipitation on surrounding air and cooling of the air as precipitation evaporates leads to the formation of down-draft (Fig. 2.4), which is particularly interesting for offshore companies. The descending air reaches the sea's surface, spreads out and forms a front strongly gusting wind which advances in the direction of the storm (Santala et al., 2014[33]).

The squall seasonality is linked to the northwards passage of the Inter-Tropical Convergence Zone (ICTZ) in the northern hemisphere during spring, then southwards in the northern hemisphere autumn in West Africa (Alvarez et al., 2011[1]). The nature of wind squall events is fundamentally different than that of high latitude non-cyclonic storms and tropical cyclones

which are presently the only types of wind events specifically addressed by API and ISO standards (Santala et al., 2014[33]).

Squalls are an integral part of the cumulonimbus lifecycle. The nature and severity of the squalls depend on the activity of the cumulonimbus storm which occurs. Cumulonimbus events over the ocean, lead to fluctuations, in low level properties (temperature, humidity and winds) which can allow subsequent systems (including ‘daughter cells’) to develop more easily on timescales of an hour or so. Inversely, the effect of widespread cumulonimbus convection is ultimately, over a period of several hours, to stabilise the atmosphere, making subsequent events less likely (Parker, 2004 [31]).

The satellite and hindcast data reproduce sustained wind speeds and directions quite well, but local perturbations such as squalls are only captured by on-site measurements by a wind sensor. Indeed, satellite data does not provide information about squall, as there are not at all stationary events: only measurements with a sampling acquisition period of at least 1Hz may enable to derivation of squall wind speeds with adequate accuracy.



*Fig. 2.3: Squall Regions (McPhail, 2014[27])*

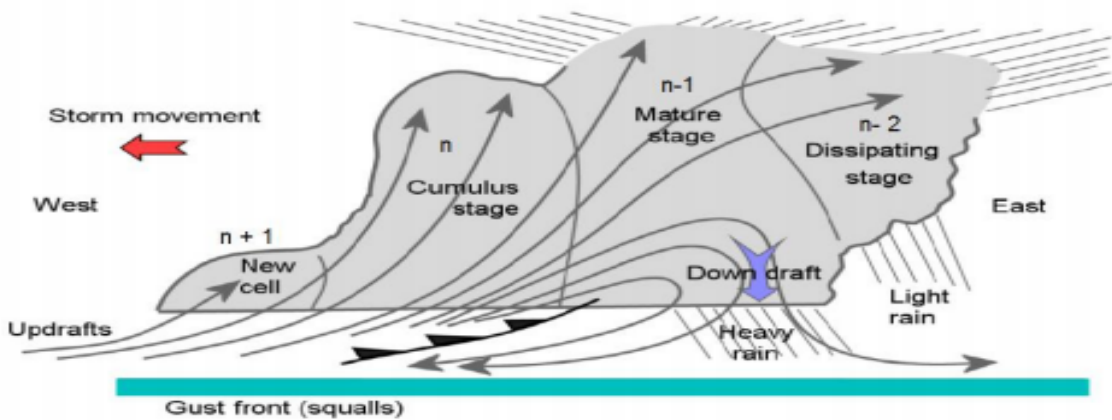


*Fig. 2.4: Squall formation and structure (Fugro GEOS, 2004[16])*

## 2.4 Overview of Shuttle Tanker-FPSO Offloading

FPSO are the dominant floating systems used to produce, store and offload oil and gas on a field. In the Gulf of Guinea, there are few floating systems such as FSO which are situated Offshore in Nigeria in a tandem offloading configuration. In general, there are two types of FPSO offloading system:

- Riser and Pipeline offloading, where the oil or gas is transferred from the platform to the shore by submarine riser and pipeline.
- Tanker transportation, mostly used in FPSO offloading, where oil is directly offloaded from FPSO to the shuttle tanker or barge which transports it to the shore.

FPSO and shuttle tankers have three types of mooring: tandem, side-by-side and buoy offloading. Tandem offloading operation is carried out in such a way that the shuttle tanker is located in the sheltered region behind FPSO (fig. 2.5a), while a side-by-side offloading operation is carried out in parallel positions. The offloading buoys are typically located 2 Km from vessel, the flowlines (generally flexible or steel pipe) run in a suspended catenary between the FPSO and the offloading buoy. The mooring systems are constructed of chain or polyester with some anchors legs (fig. 2.5b). Compared with side-by-side mooring, tandem mooring can withstand more rigorous environmental conditions and is more advantageous faster disconnection. The mooring system connecting the FPSO to the seabed can be either in spread or Single Point Mooring (SPM, as the FSO). Generally the vessels are connected to each other either by a single hawser or by a couple. Use of thrusters, tug or main engine can reduce instabilities and large relative headings.

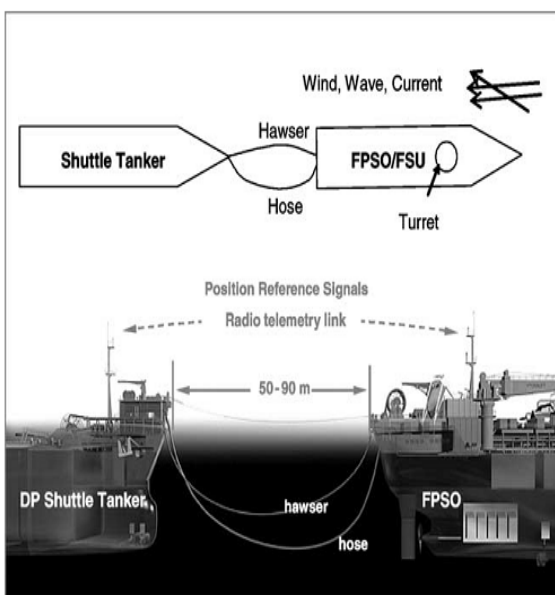


*Fig. 2.5: (a) Shuttle tanker tandem offloading from FPSO (Chen & Moan, 2003 [10])*



*Fig. 2.5: (b) Offloading from a deepwater offloading buoys (Duggal & Ryu 2005 [13])*

## CHAPTER 3

# Study Area, Data Acquisition and Methodology

## 3.1 Study Area

This study is centred on a FSO (Fig.3.1.b) and on a oil platform (Fig.3.1.c) offshore in the Niger Delta area of the Nigerian Continental Shelf (West Africa, Gulf of Guinea). This FSO receives crude at a rate of 230,000 barrels per day from different Fields. It has a capacity to store 2.2 millions barrels of crude oil and has an overall length of 300m, a width of 62m and a depth of 32m, with dead weight of 341,000 tons. It has external turret.



*Fig. 3.1: Study location, FSO and Oil Platform, Offshore Nigeria [37]*

The oil field is under the influence of semi-diurnal tides with meso-tidal range between 2-4m, which propagate up to the coast in a south westerly direction (Ojinnaka, 2006, [28]). The wave height varies from 0 to 4m, the main current which dominates is the West-East Guinea Current, with a mean current speed of 0.3 m/s . At this area, the sea surface temperature ranges from 27-28°C during the dry season and 24-25°C during the rainy season. The salinity varies from 27 to 30 psu depending on the season and the main rivers which feeds the field are the Bonny and Niger Delta rivers.

The deformation and nonlinear interaction of the  $M_2$ <sup>1</sup> and  $S_2$ <sup>2</sup> internal tides in the Nigerian Continental Shelf which have particular bathymetry and stratified water leads to a generation of solitons and their propagation at the field (Clarke & Battisti, 1983 [11]). Commonly called the ‘*Rip Tide*’ in marine jargon, solitons encounter in West African shelf break. In comparison with the Andaman Sea, South China, Canadian Sea and the Gulf of Mexico, West African offshore are not yet well documented in Internal waves studies.

The climate of the study region is dominated by the West African Monsoon (WAM), which is, in turn, closely tied to the seasonal movement of the Inter-Tropical Convergence Zone (ITCZ), resulting from the convergence of trade winds from the North-East and from the South-East, and which are characterised by a great activity of cumulonimbus vertical formation and by heavy rains and squall (Legerstee et al., 2006 [26]). The Saharan Air Layer (SAL) is a very dry layer of air which lies above the humid oceanic air and monsoon air, and plays an important role in squall occurrence. The dryness of the SAL is essential for the development of intense downdraught, because it allows intense evaporative cooling (Parker, 2004 [31]).

The climate of this region is also same scheme of the tropical climate; the rainy season falls between April and October (with the highest rainfall on June) and dry season between November and March. During the rainy season, there are a mean annual rainfall of 2540-4060 mm (Dublin-Green et al., 1999 [12])  $ms^{-1}$ . Mean wind speed of 4.5 to  $5.1\ ms^{-1}$  are usually recorded at this region when mean wind direction ranges from 161 to about 190 degrees (Jimoh, 2010 [25]).

## 3.2 Data Acquisition

In this study, we used the in-situ data taken on a Oil Platform and on a FSO. The in-situ data was collected from 13 March 2013 to 29 August 2014. We have devised the data collection into two parts: the first part of data was collected on a platform and the second part was collected on FSO.

### 3.2.1 Oil Platform Data

The ADCP is an upward looking Teledyne 300kHz ADCP, located on the 17.5m level of the oil platform bridge and deployed at a depth of approximately 30 meters below the waterline depending on tide and sea level. It gives current speeds, direction through the water profile, sea temperature at ADCP level, Pitch, Roll and Heading (Fig.3.2). It provides measurements with 2m bins length and 1 minute of temporal resolution.

The wave sensor is installed at the same location as the ADCP on the bridge of oil platform and mounted at 18.32m above MLS (Mean Sea Level). The sensor is Rex Wave Radar SAAB, and it gives us the characteristics of waves such as their height and period, and the water level tidal height which allows to quantify the correlation between the tidal cycle and soliton occurrence.

---

<sup>1</sup>The Principal Lunar semi-diurnal constituent

<sup>2</sup>The Principal Solar semi-diurnal constituent

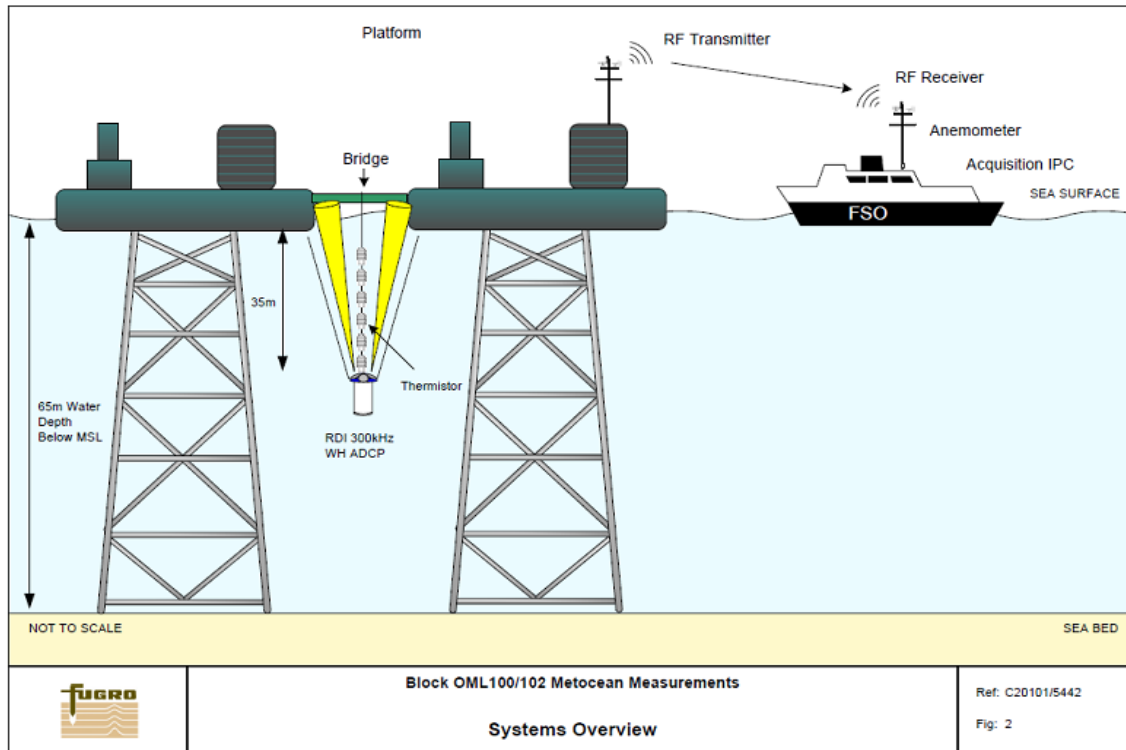


Fig. 3.2: Overview of metocean data acquisition system

### 3.2.2 FSO Data Collected

The wind data are taken by a wind sensor mounted on board the FSO approximately 72m above MLS. The sensor installed is an RM Young Monitor Marine Anemometer.

The FSO position is taken by a GPS located in enclosure antenna. The accuracy of the GPS data is decimetre (from Fugro G2 solution, RTK float). GPS data of FSO are analysed taking as reference the first FSO position of each plot. During the loading of a Tanker (with buoy Tandem), mooring Hawser tension data are collected.

## 3.3 Methodology and Data Analysis

The methodology which we employed is based on the profiling and statistical analysis of the in-situ dataset. We did our analysis within the time series data issued from the ADCP and the wave sensor taken on a oil platform and the data taken on FSO. We first made a quality control of data taken from 12 March 2013 16:05 to 17 May 2013 15:21, from 24 July 2013 09:50 to 31 December 2013 09:32 UTC and from 01 January 2014 00:04 to 27 August 2014 11:20 UTC.

### 3.3.1 Data Quality Control

The objective of data quality control is essentially "to ensure the data consistency within a single data set and within a collection of data sets and to ensure that the quality and errors of the data are apparent to the user who has sufficient information to assess its suitability for a task (IOC/CEC Manual, 1993 [22]).

Our set data is more complex with many mixing, doubtful and bad values. There are done some treatments of these data. For current speed, we have removed the negative values and higher ( $> 1.5 \text{ ms}^{-1}$  for example due to noise or to other phenomenon) values. We have taken current directions and heading deviation between 000 and 360 °T. We have also deleted the 12<sup>th</sup> bin because it is much closer to the sea surface where the quality of data is not good. Finally, we have removed the tidal height data higher to 1.8m to be in agreement to the characteristics of tidal height in this area.

We have removed the value less than 20 T in hawser tension data, to take only the offloading period between the tanker and FSO. The wind data are no got some problem, we have taken only the direction interval between 000 and 360 °T. Quality control had been done on GPS data and heading that we used. All this control are doing to remove the absurd values which can be due to a poor response of the apparatus or due to other phenomenon.

### 3.3.2 Soliton identification

Solitons are very short lived phenomena. They are ranked among the high frequency oceanographic events. Solitons can be detected by sudden variation and strong current speed and direction. Solitons are also associated with oscillations of thermocline characterized by temperature change and ADCP pitch and roll opposite tilt. We identify the horizontal currents associated with solitons by removing longer duration fluctuations caused by other low frequency oceanographic processes. This analysis was done by subtracting a three hour running mean from the one minute horizontal velocity data. We used an existing screening algorithm developed by Fugro to identify all potential soliton events:

1. Using a depth integrated high frequency speed squared in order to minimize the small magnitude and bring out the magnitudes corresponding to soliton events by setting threshold;
2. Use of a minimum peak separation time of 6 minutes to isolate individual solitons.
3. In addition a threshold was a setup on Pitch, Roll and Temperature from the ADCP data to see any variation due to soliton passage.

### 3.3.3 Squall identification

Squall events were objectively identified based on the widely used definition by the World Meteorological Organization (WMO, 1962 [35] ): 'A sudden increase of wind speed by at least  $8 \text{ ms}^{-1}$ , rising to  $11 \text{ ms}^{-1}$  or more and lasting for at least one minute.' Sudden was not defined in exact terms, but in this study it was chosen to be within no more than 10 minutes (as used by Berkes et al., 2012 [6]). We developed a screening algorithm to identify all candidate squall events as:

1. Setting a threshold on wind speed data;
2. Setting a maximum time interval during which the wind speed increases suddenly.
3. Using minimum peak separation time of 1 hour.

### 3.3.4 Analysis of FSO and Tanker Responses

Sudden increase of speed (in wind and sea current) and changes direction (in wind and sea current) will have a significant influence on the behaviour of the shuttle tanker, and dynamic effects will be prevailing, not only in terms of tension in the mooring lines or in the hawser but also in terms of relative heading.

The dynamic response of FSO and Tanker are studied by making a careful analysis on GPS and heading data of FSO as well as on the hawser tension data during the loading period of the shuttle tanker.

During the passage of squall and/or soliton events, the FSO rotation can be seen by the heading change. The position (displacement or rotation) of FSO was investigated through the analysis of GPS data. We have:

- subtracted the reference position data to all GPS data; Here we have taken the data of first position of tanker period as reference. But in the absence of tanker, the first position of each plot (in unique case of FSO response) is taken as reference.
- Converted the geographical coordinates into distance, using the Matlab functions.

The response of shuttle tanker during these phenomena was investigated by the plot of the time series of hawser tension data.

When shuttle tanker is in taut hawser mode and during the passage of squall and/or soliton events, hawser mooring can be broken, and/or position of FSO and shuttle tanker can change. The rise time (duration of increase of wind speed) of each squall event was examined to evaluate the critical period during which the squall will have much more influence on the shuttle Tanker and on FSO.

Generally, the response of vessels and shuttle tankers to squall and/or soliton events depends on parameters such as the: intensity of the event (power and speed), the direction of the event, the duration of the event and the positioning of the FPSO/FSO - Shuttle Tanker type.

In this study, all Shuttle tankers that came to transport oil at this location were connected in tandem configuration to the FSO system through bow or starboard hawser, during the offloading process.

---

CHAPTER 4

---

# Results and Discussions

---

The arrival of extreme soliton events on the system from the bow or starboard can impact tandem and/or lead to the change of heading and can bring about an increase of hawser tension. The arrival of a squall event on this FSO can lead to a change of FSO position and heading.

## 4.1 Soliton

The detailed characteristics of the observed solitons are examined for all periods of data acquisition.

### 4.1.1 Case Analysis

Figure 4.1, figure 4.2 and figure 4.3 show the colour contour and plot of the measured current speed (filtered and unfiltered velocity, direction, maximum speed and depth integrated speed), Pitch, Roll, Temperature and Tidal height of 23th May 2014. This case analysis was chose due to characteristic and frequency of soliton groups on this day.

That day, soliton groups recur with interval time of 12 hours 50 minutes relative to the semi-diurnal tidal cycle in this area. Two soliton groups were observed exactly between 04:40 and 06:20 UTC, and between 17:30 and 19:15 UTC. The temperature, ADCP pitch and roll, and tidal height structures show how the passage of solitons is associated with the semi-diurnal tidal cycle. These ones occur in low tide period.

The first soliton group is presented in more detail in figure 4.4, figure 4.5 and figure 4.6. The direction of solitons group can be found from the sign of Northward and Eastward velocities. Northward velocity contour plot shows that the soliton moves towards the north in the water column. Eastward currents contour plot shows that between 13 and 17 m of water depth, soliton packet moves towards the east, while in the upper layer and between 18 to 25 m it moves towards the east. The pitch and roll plots show the arrival of 6 individual waves exactly at 04:40 UTC, with 12 minutes between the first and the second wave, and about 7 minutes of time separation between the others. The maximum speed of soliton is founded by searching the maximum speed over the depth (11 bins). During the passage of this soliton packet, the maximum speed of an individual wave is about  $0.4ms^{-1}$ . The current direction is determined from the depth (bin) corresponding to the maximum speed. In this case, the current direction of soliton is approximately to the North-North-East ( $29^{\circ}T$ ).

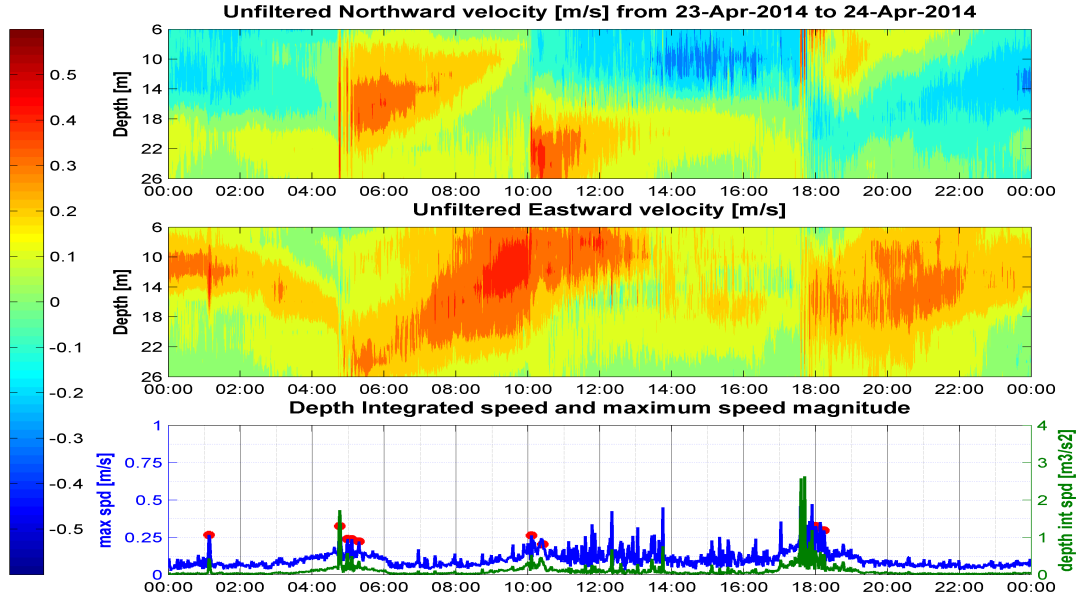


*Fig. 4.1:* 24-hour of unfiltered Northward and Eastward velocities, maximum speed and depth integrated speed observed on 23 April 2014, showing two solitons events.

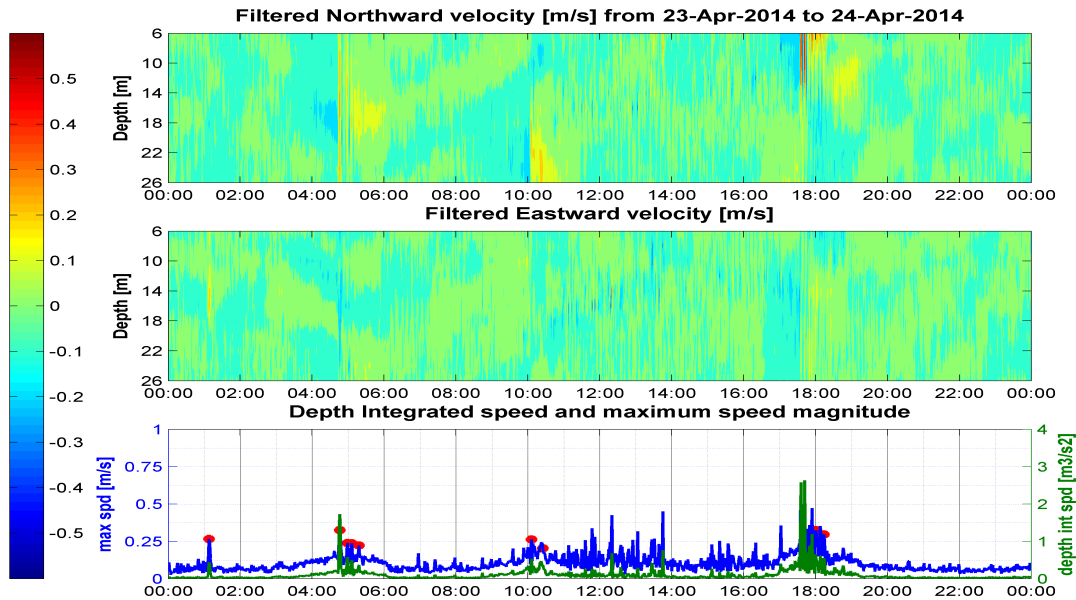


*Fig. 4.2:* 24-hour of Filtered Northward and Eastward velocities, maximum speed and depth integrated speed observed on 23 April 2014, showing two solitons events.

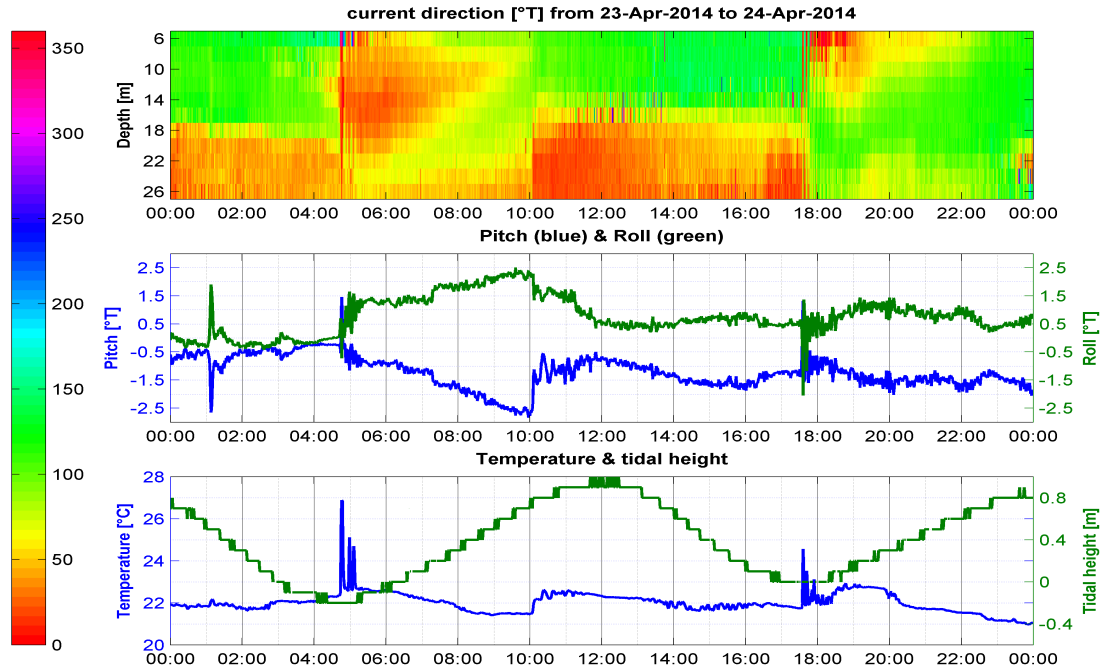


Fig. 4.3: 24-hour of Current direction contour, ADCP pitch and roll, Temperature and tidal height observed on 23 April 2014, showing semi-diurnal soliton occurrence.

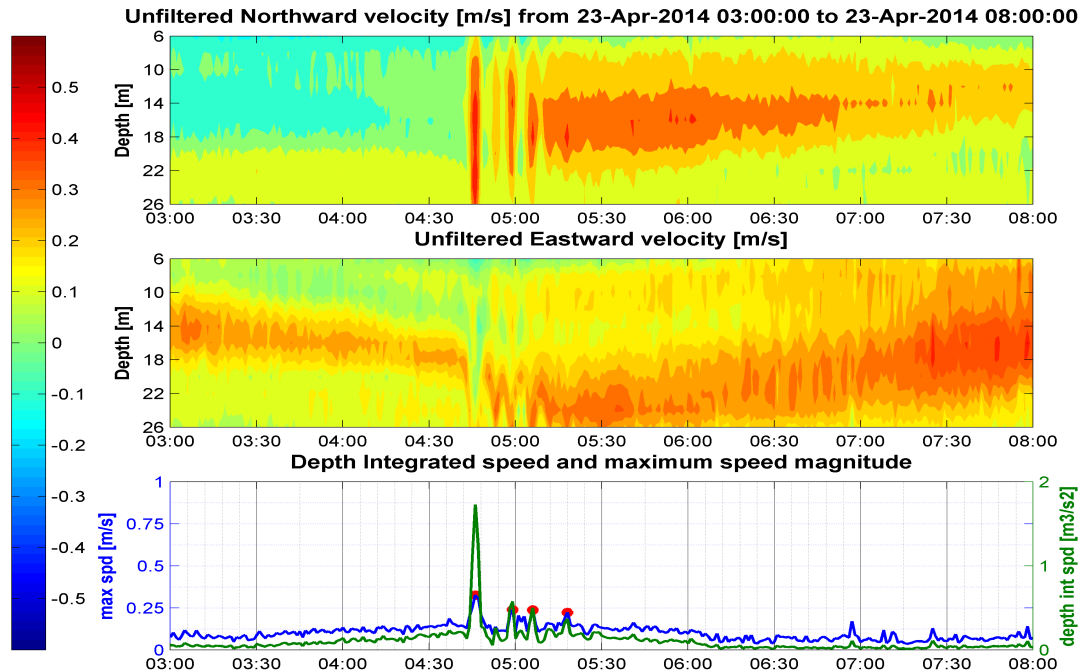


Fig. 4.4: 4-hour of unfiltered Northward and Eastward velocities, maximum speed and depth integrated speed observed on the 23 April 2014, showing one soliton event at 04:45 UTC.

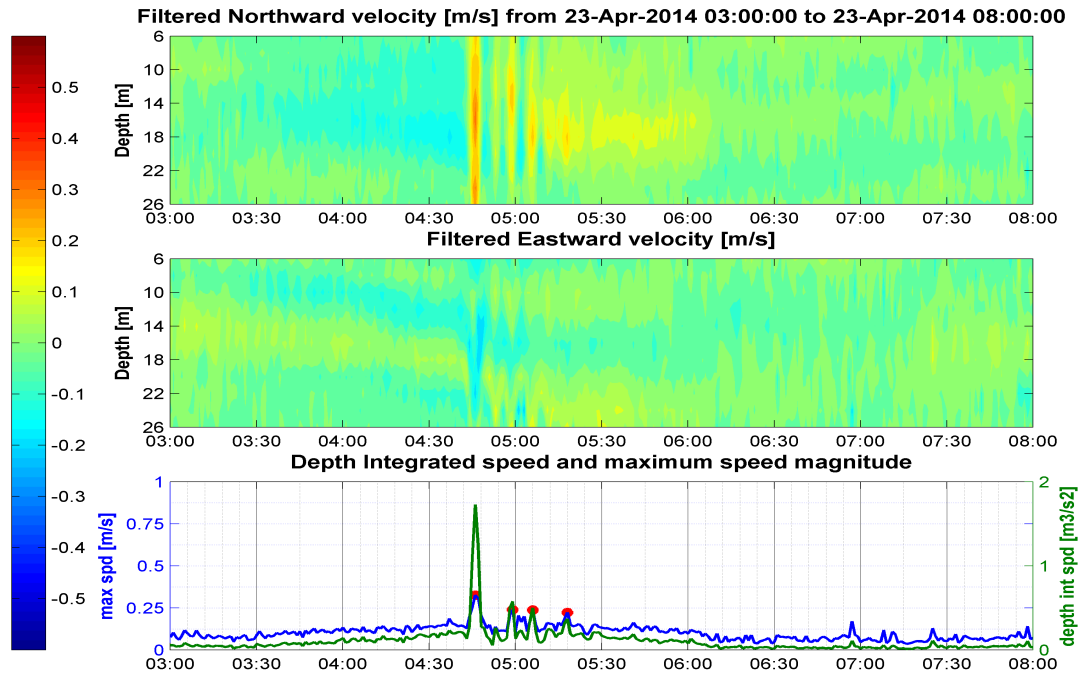


Fig. 4.5: 4-hour of Filtered Northward and Eastward velocities, maximum speed and depth integrated speed observed on the 23 April 2014, showing one soliton event at 04:45 UTC.

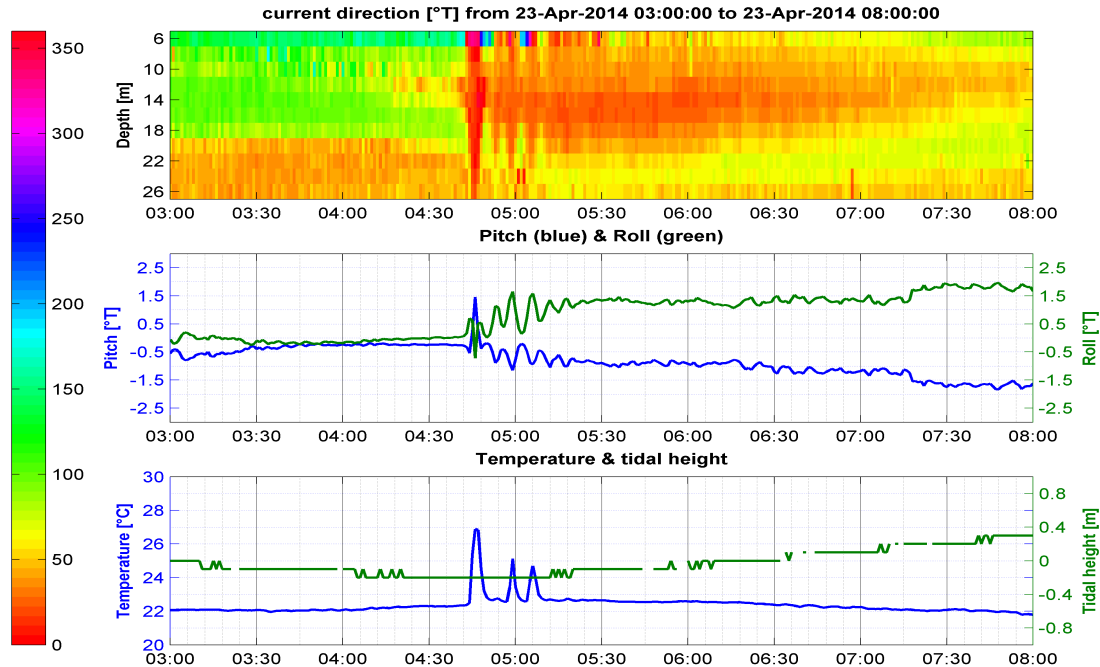
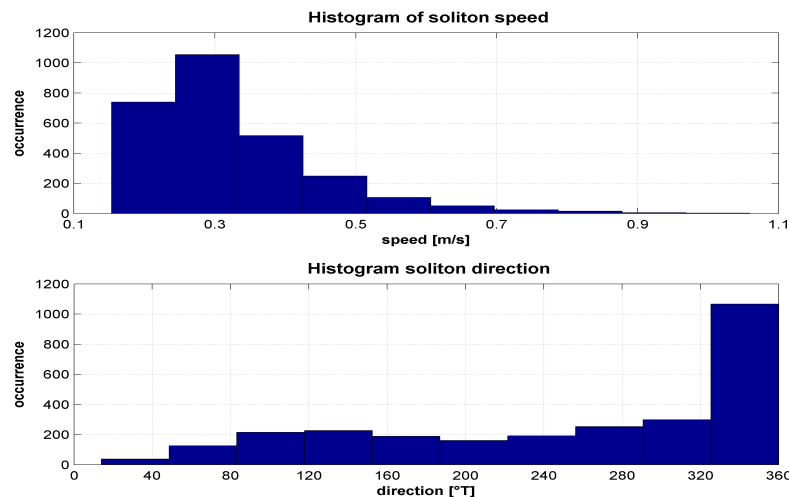


Fig. 4.6: Current direction, ADCP pitch and roll, Temperature and tidal height plots observed on the 23 April 2014 04:45, showing solitons packet.

### 4.1.2 Solitons Statistics

At this location, 2761 individual solitons were identified over the period (463 days) with 273 soliton events (soliton packets). Overall, of the 273 events, 96 events with semi-diurnal frequency (two events per day) were identified and with an average period of 12 hours 47 minutes at oil platform area. The frequency of these events is relative to the semi-diurnal tidal cycle in this area (Gulf of Guinea). Generally, the time lapse between the first high individual wave and the next of soliton packet is approximately 7 to 12 minutes. The average duration of propagation of a soliton event is 1 hour 45 minutes at this location. Overall, of the 273 events, 124 occurred at periods of high tide while 149 occurred at periods of low tide. At this location, the link between the occurrence solitons and semi-diurnal tide cycle is quite approximative, because we found some days with a single soliton event and some days without an event.

Figure 4.7 which presents a histogram of soliton (speed and direction) occurrence shows that the main direction of current speed is to the North-North-West ( $350^{\circ}\text{T}$ ) and the speed of maximum soliton occurrence is  $0.35 \text{ m/s}^{-1}$ . The monthly frequency of soliton occurrence is given by the table 4.1.1 where we can notice that solitons occur mostly in April 2013, also between November 2013 and February 2014, and in April 2014, but less in March and from June to August (boreal summer).



*Fig. 4.7: Currents speed (top) and direction (bottom) associated with observed soliton.*

Table 4.1.1: Monthly occurrence of soliton events. MD: Missing Data

	Jan	Feb	Mar	Apr	May	Jun	Jul	Aug	Sep	Oct	Nov	Dec
<b>2014</b>	32	19	11	24	17	13	16	14	MD	MD	MD	MD
<b>2013</b>	MD	MD	11	18	10	MD	5	14	14	16	20	19
<b>Total</b>	32	19	22	42	27	13	21	28	14	16	20	19

### 4.1.3 FSO and Tanker response during an extreme soliton event

Figure 4.8.a presents the time series plots of current speed and temperature showing the passage of soliton packet at oil platform between 04:30 and 05:45 UTC on 24 April 2014. We can note the peaks of current which reach  $0.4 \text{ ms}^{-1}$  and a temperature variation of  $2^\circ\text{C}$ . The response of FSO is shown by figure 4.8.b, whereas we can see a higher variation of FSO displacement. There are also observed the change of heading from  $320$  to  $240^\circ\text{T}$  from 06:35 to 07:45 UTC. Since the plots of FSO heading and displacement are uncorrelated at this moment, we can tell that the FSO has deviated and has also moved. Figure 4.8.c shows the time series plot of mooring hawser tension showing the response of the shuttle tanker. During the passage (on the 24 April 2014) of this soliton event on FSO-shuttle tanker system, the hawser tension increases quickly and reaches 235 tons in 18 minutes and with five peaks higher than 100 tons, which is enormously dangerous for the hose. The mean duration during which the hawser is affected by these events is approximately 2 hours.

From a daily FSO log showing rip tide record, response of FSO and tanker, and action taken by personnel, it is noted that the hose was disconnected and loading of tanker was suspended for 3 hours due to the violent response of the tandem that day. Some cases of shuttle tanker response during soliton events are presented in appendix 5.2.

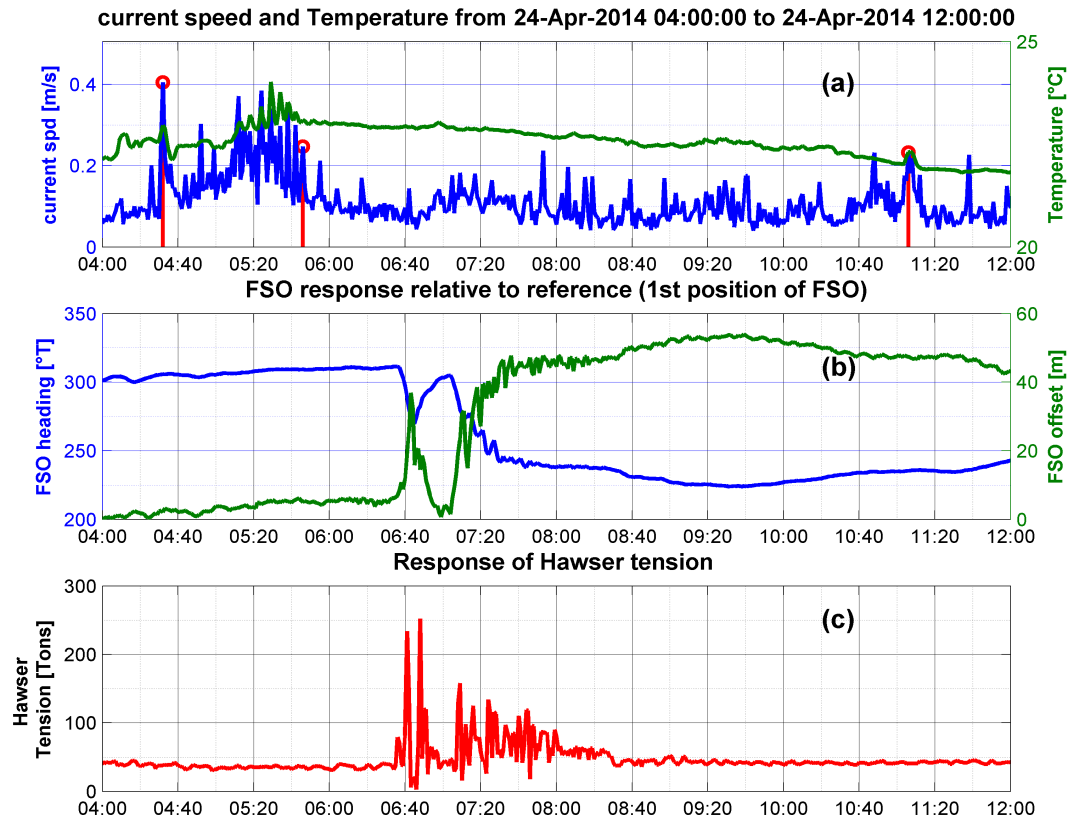
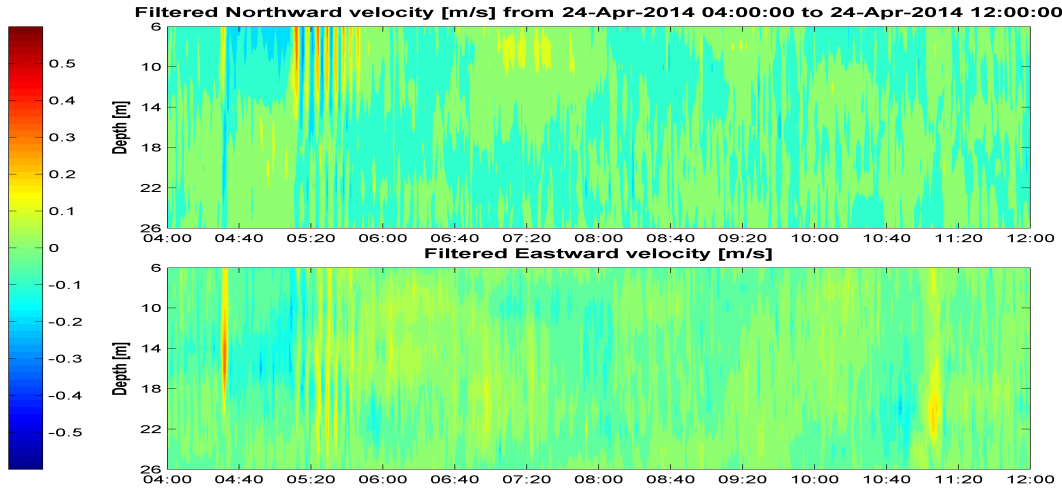


Fig. 4.8: Current speed, FSO displacement and heading, and hawser tension.



*Fig. 4.9: Contour plots of filtered Northward and Eastward velocity.*

#### 4.1.4 Analysis of Broken Mooring Hawser Case

Friday, December 20, 2013 there was a strong soliton (fig. 4.10) event that occurred on the oil platforms at 13:30 UTC and on FSO at 14:30 UTC, with a speed that reached  $0.85 \text{ ms}^{-1}$ . Figure 4.11.b shows that the heading change from 0 to  $320^\circ \text{T}$ . The FSO position is not displayed as there was no GPS data available during this period. The response of the shuttle tanker was violent and led to the breaking of the mooring hawser, as shown on figure 4.11.c, but the hose was disconnected on time. On this figure, we can see a quick increase of up to 165 tons of hawser tension in 5 minutes, and suddenly (exactly at 14:40) it reduces to zero. The travel time of the soliton event from oil platforms to FSO was around 1 hour, whereas the mean travel time of all soliton events is about 1 hour 45 minutes; so it was very fast with very high energy.

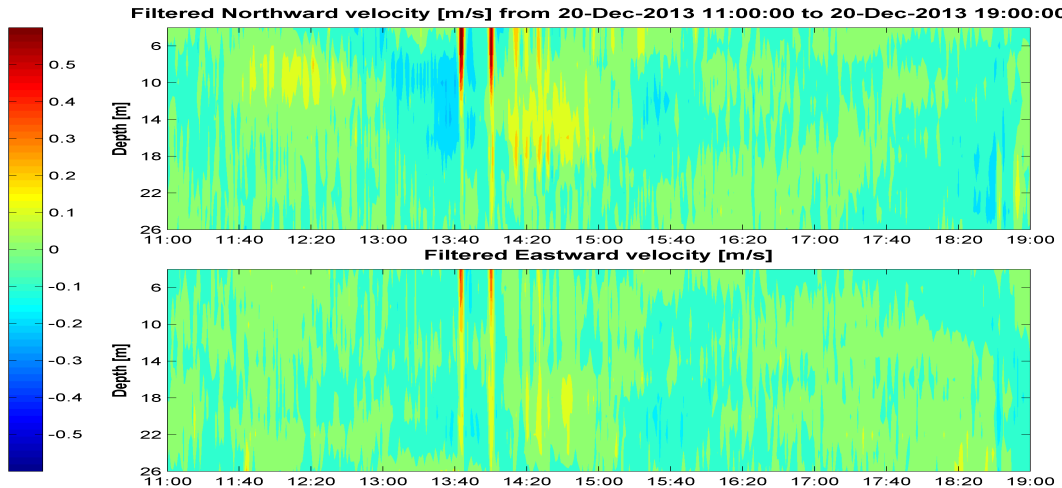


*Fig. 4.10: 8-hour contour plots of filtered Northward and Eastward velocity showing a strong soliton event*

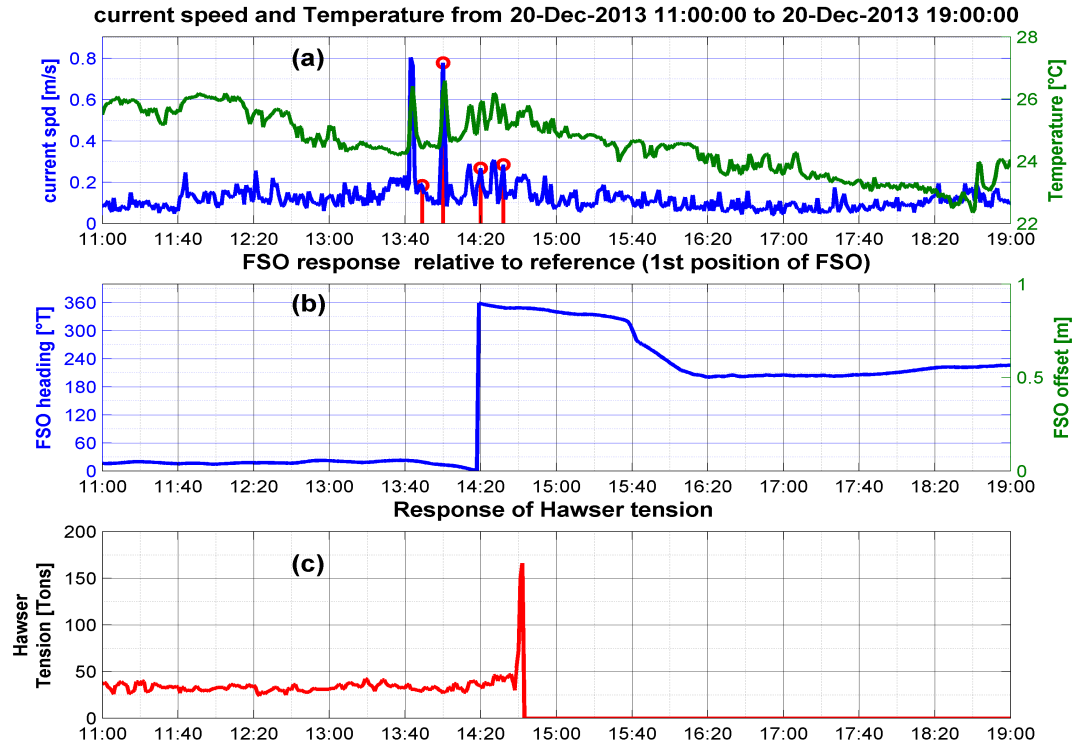


Fig. 4.11: 8-hour plots of current speed and temperature, heading of FSO and Hawser tension, showing the breaking of mooring hawsers due to strong soliton event

## 4.2 Squall

Squall events at any area, are usually characterized by the rise time, wind speed and direction, the frequency of occurrence, air temperature, specific humidity, precipitation and pressure. Any correlation with other atmospheric and oceanic phenomena can also be quantified.

In this study, only rise time (time from which wind speed begins to increase to maximum speed), wind speed and direction, the frequency of occurrence (founded) were used as characteristics.

### 4.2.1 Case analysis

An example of a mesoscale squall event on 25 March 2014 is given in Figure 4.12. The event hit the FSO around 08:35 UTC with a wind speed which reaches up to  $19.5 \text{ ms}^{-1}$ , increasing rapidly from  $3-12.5 \text{ ms}^{-1}$  in just a few minutes. The wind direction changed from West to East-North-East with the arrival of the squall. Just before arrival of squall, wind speed decreased of  $5 \text{ ms}^{-1}$  in about 1 hour 30 minutes. Wind speed then decreased gradually from 16 to  $2 \text{ ms}^{-1}$  around 45 minutes after the passage, which in accordance with theory: after the passage of a squall event, there is an extension of the cold pool. The rise time for this squall event is about 20 minutes. This event is an extreme case; the increase of wind speed is very large and the change of wind direction is quite brutal.

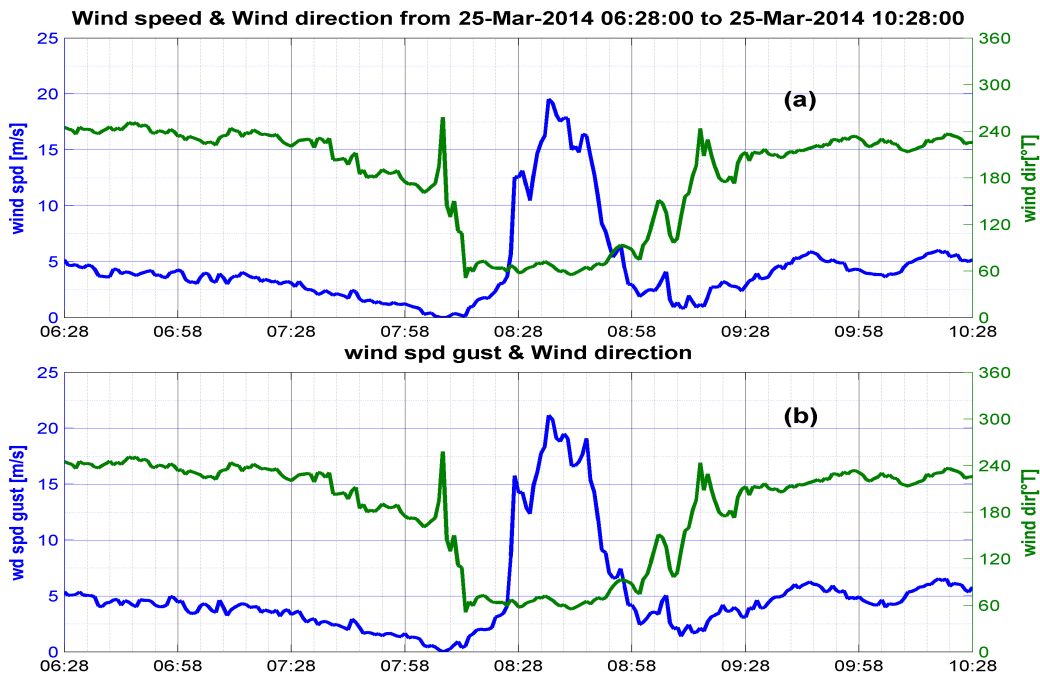


Fig. 4.12: Wind speed and direction (a), wind speed gust and direction (b), showing the passage of squall event on 25 March 2014.

#### 4.2.2 Squall statistics at FSO

From the analysis of these wind data, 95 squall events were identified over the 463 days of data collection. Table 4.2.1 shows the distribution of squall events during the years 2013 and 2014. There are no data from mid-May to mid-July 2013, but there are many more events in April 2013 and from April to June 2014. We note the absence of squall events in July 2013 and August 2014, which corresponds to the rainy season.

The Squall occurrence relative to wind speed and direction are given by the figure 4.13. We can note that the main maximum wind speed of squall events in this area is about  $11.5 \text{ ms}^{-1}$ . The squall direction varies greatly but with mainly direction from South-West. The mean rise time of these events is about 14 minutes.

Table 4.2.1: *Monthly occurrence of squall events. MD: Missing Data*

	Jan	Feb	Mar	Apr	May	Jun	Jul	Aug	Sep	Oct	Nov	Dec
<b>2014</b>	3	7	7	10	10	10	1	0	MD	MD	MD	MD
<b>2013</b>	MD	MD	5	10	5	MD	0	3	7	5	6	6
<b>Total</b>	3	7	12	20	15	10	1	3	7	5	6	6

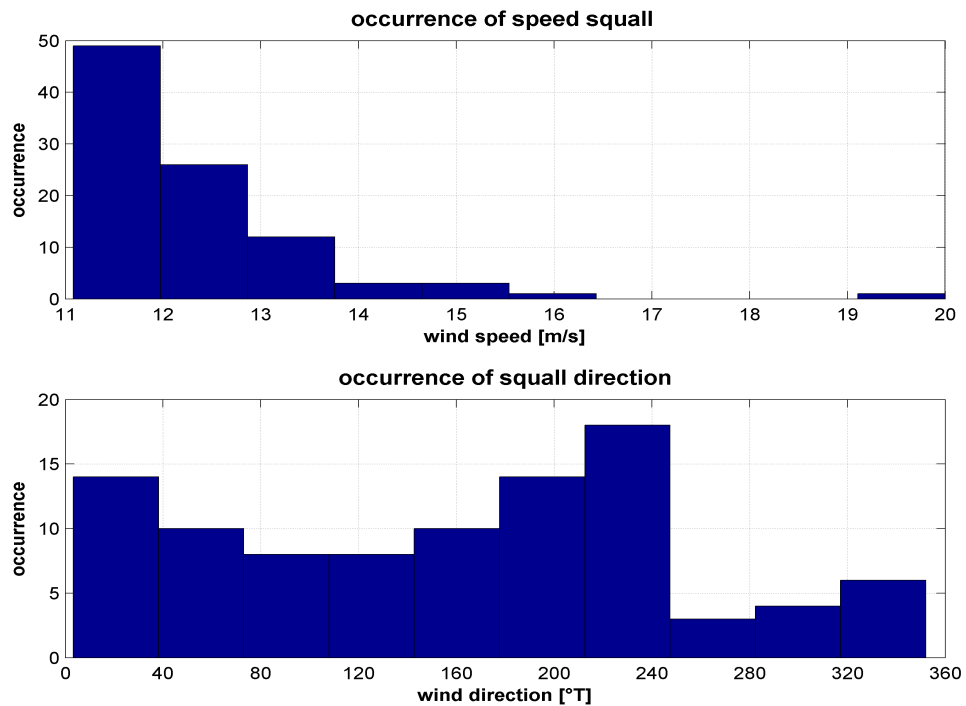


Fig. 4.13: Occurrence of squall relative to wind speed (top) and to wind direction (bottom).

#### 4.2.3 Annual and Diurnal Variation

Concerning the frequency of squall events at this location, figure 4.14 above gives a few cycles and shows the average monthly distribution of squall days. There are no data from mid-May to mid-July 2013. We can note many more events per month from April to May, where the number of squall reaches 15 or more. But, there are very few (almost inconsiderable) events from July to August, which corresponds to the rainy season in Gulf of Guinea. Squall occurrence at Offshore Nigeria is considerably influenced by the displacement of ITCZ. During the boreal summer, ITCZ is above the Sahelian zone, atmospheric conditions are very stable. Thus, there are less squall events, but we have many events during the spring, where ITCZ moves from the south towards GG and during autumn where ITCZ moves from GG (Equator) towards the North. Therefore, the squall events have an annual cycle in offshore Nigeria.

The diurnal cycle of tropical convection is an important feature in the understanding of the dynamics of the initiation, organisation, and propagation in the absence of synoptic-scale control(e.g., Yang & Slingo, 2001 [36]). Figure 4.14 shows the diurnal distribution over 3-hour interval of squall event. We can note the maximum activity between 06:00 and 09:00 and between 21:00 and 23:59 UTC. Squall occurrence quickly falls off toward the afternoon and the mid-night. This diurnal cycle of these events is more difficult to interpret, but it can be linked to the process of convection over land in the afternoon (Jackson et al., 2009 [23]) or to the propagation of river Niger over the ocean.

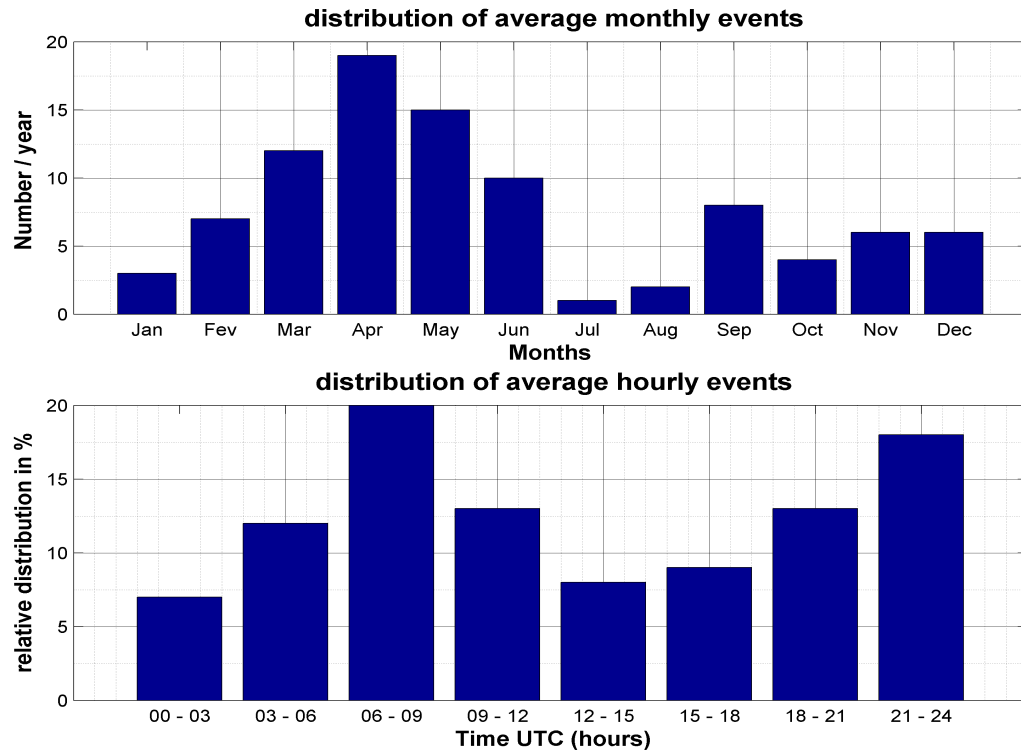


Fig. 4.14: Distribution of average monthly squall event over the two years (top) and diurnal distribution in % for 3-hourly intervals (bottom).

#### 4.2.4 FSO response during an extreme squall event

The response of FSO to a squall event is proportional to the wind speed and direction. Figure 4.15.a presents time series plots of wind speed and direction, showing the passage of a squall on 23 February 2014 between 00:45 and 03:00 UTC. The wind speed increased from  $7 \text{ ms}^{-1}$  to  $18 \text{ ms}^{-1}$  in 20 minutes and the direction changed from  $260$  to  $320$  °T. This is an extreme event. The response of FSO is shown by figure 4.15.b, where we can note heading change from  $260$  to  $340$  °T. We can remark a good correlation between FSO heading and displacement plots; Thus, the FSO has not displaced, but it has just rotated. More response of FSO to some squall events are given in appendix 5.2

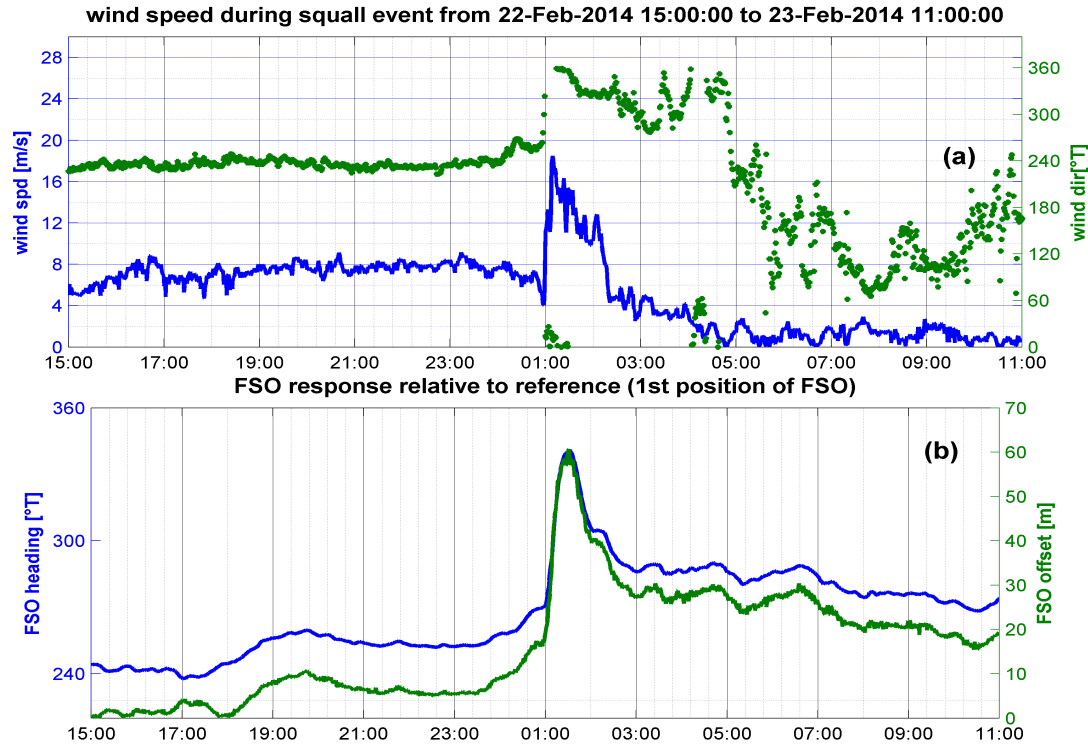


Fig. 4.15: 20-hour time series plot of FSO rotation and heading showing FSO response during a squall event on 23 February 2014.

## 4.3 Discussion

### 4.3.1 Predictability of soliton events

Soliton prediction can be done by means of two different approaches:

- Soliton prediction centred on the KDV equation (2.2.1) which does not predict their formation, but provides minimum criteria for solitons to propagate and develop. It is based on the prediction of KDV parameters combined with current/tidal model data and enables forecasts of solitons to be made. Such a system is the basis of an early warning system being developed by the US Navy (Ramp, 2006 [32]) for the northern part of the South China Sea.
- Analysis of measurement data (tidal and current) in order to yield statistical correlations to other environmental variables. These correlations might then be used as the basis of an early warning system. This method was used in this work to analyse correlation between soliton occurrence and tidal cycle.

The tidal range for the tidal cycle (LW to HW) was determined from the analysis of the observed elevation in water level. The tidal ranges occurring during each tidal cycle were grouped into 0.2m bands, the number of occurrences of tidal range and soliton occurrence within each band were calculated. From these values, the probability of soliton occurrence was given by the relation 4.3.1. The results obtained through the data taken from 12 March 2013 16:05 to 17

May 2013 15:21, from 24 July 2013 09:50 to 31 December 2013 09:32 UTC and from 01 January 2014 00:04 to 27 August 2014 11:20 UTC are presented in Table 4.3.1 . In principle and for Offshore operation, a line can be drawn at the tidal range threshold corresponding to any soliton occurrence probably. For example, there is less than 35% chance to have soliton occurrence for a threshold tidal range of 2 m in this area.

$$\text{Probability of Occurrence} = \frac{\text{Number of Soliton Occurrence}}{\text{Number of Tidal Occurrence}} * 100 \quad (4.3.1)$$

Table 4.3.1: *Occurrence of Soliton with Tidal Range over the data acquisition period*

Tidal Range LW to HW(m)	N° occurrence Tidal Range	N° occurrence of Solitons	Ptg occurrence of Solitons (%)
<1	180	50	28
1 to 1.2	155	50	32
1.2 to 1.4	151	44	29
1.4 to 1.6	160	48	30
1.6 to 1.8	165	50	30
1.8 to 2	60	18	30
> 2	49	13	27
<b>Total</b>	<b>920</b>	<b>273</b>	<b>30</b>

### 4.3.2 Soliton

This study has confirmed the occurrence of solitons at this field. There are 273 recorded solitons events, with 96 of semi-diurnal frequency. During three months of data taken by Fugro GEOS at Offshore Myanmar, it was found that solitons of significant amplitude were only observed during spring tides when the tidal range exceeds 1.5 m. They have also founded that the percentage of soliton occurrence is greater when the tidal range is larger (Hyder et al., 2005[20]). Here according to previous study at this location (Fugro GEOS, 2010 [17]) we have founded that the solitons appears frequently with spring tide, before and after (figure 4.16). The mean percentage of soliton occurrence relative to the tidal range calculated previously shows that this percentage varies very slightly (27-32%). So it is unreal to use only tide to predict soliton event in this area.

The solitons were typically observed in satellite imagery between May and October 1973 in New-York Bight (Apel et al., 1975 [2]), whereas in our study soliton events are mainly observed between November and February. During this period, we have a reinforcement of Guinea current (Bourles, 2008 [7], in the northern of Gulf of Guinea which could favour the occurrence of soliton in this area.

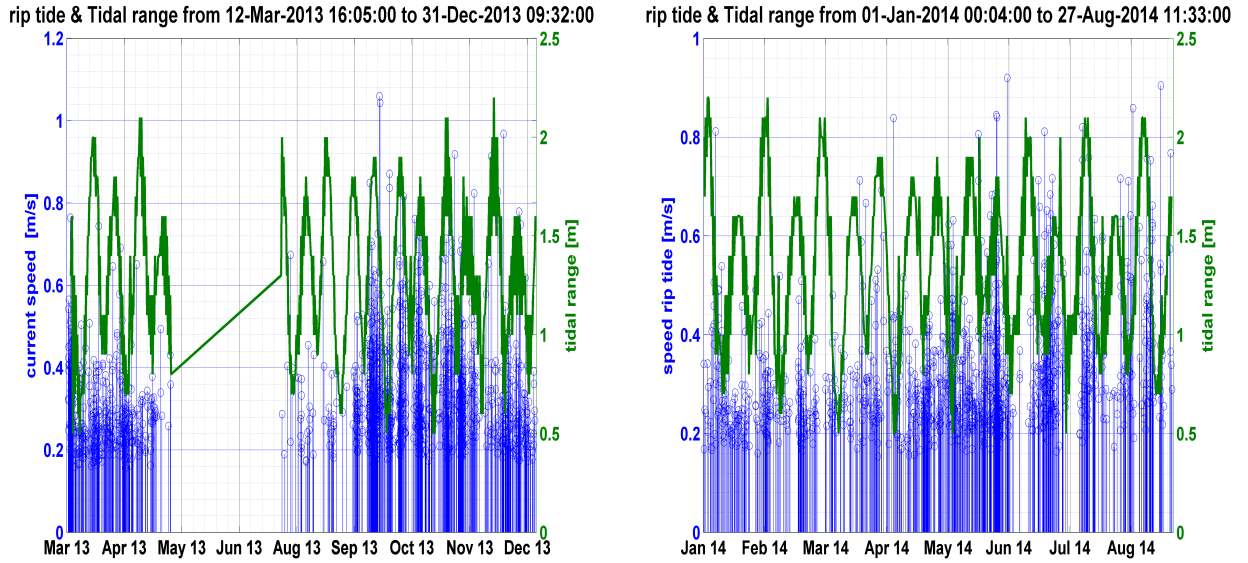


Fig. 4.16: Soliton events with tidal range from March 2013 to August 2014.

### 4.3.3 Squall

The total number of squall events (95) at this location over the 463 days of recorded data is considerably comparative to a previous study of squall events on certain towns in Nigeria from 1939 to 1941 by Hamilton and Archbold (1945[19]). They recorded 133 and 116 events at Kano and Maiduguri respectively for the years 1939-1941 (1095 days). Hamilton has noted the complete absence of squalls in July and August (rainy season) at Lagos and Calabar which agrees with our result. Berkes et al.(2012[6]) reported 32 events on an oil platform located at the Angolan enclave of Cabinda within the context of West African Gust (WAG) project over 340 days in 2007-2008, coordinated by Fugro GEOS Ltd. Three or more events per month were recorded from February to May with a diurnal cycle relatively constant.

The absence of pressure, air temperature and specific humidity data in this study can mean to an overestimation of squall events at this location; identification of squall events within these data in addition to wind data will be much more accurate.

### 4.3.4 FSO and Shuttle tanker response

Brugts and Krekel (2004 [9]) have reported an increase of hawser tension during the FPSO Munin offloading on Xijiang field (Offshore China), which reached 150 tons in 20 minutes during the passage of a soliton event. In this study, the hawser tension reaches 265 tons in 15 minutes during one soliton event and 165 tons in 6 minutes just before the breakage of the mooring hawser during another strong soliton event. The increase of hawser tension depends of the type and intensity of soliton event and also, depends of the area.

Concerning the position of FSO, Brugts and Krekel (2004 [9]) have reported that the heading range can reach up 150 °T, whereas in our analysis, there is maximum range of heading of 120 °T during a strong soliton or squall event on 23 April 2014.

---

CHAPTER 5

---

# Conclusion and Recommendations

---

## 5.1 Conclusion

After the analysis of *in-situ* data from this oil platform and FSO, Offshore Nigeria, we arrive at the following conclusion:

1. This oil field data show existence and propagation of solitons relative to the interaction between the internal tide and significant topographic features, and squalls due to some extreme atmospheric conditions;
2. The occurrence of relatively strong soliton event on 20 December 2013 at 13:30 UTC at oil platform, which caused breaking of a mooring hawser after an increase of hawser tension from 40 to 165 tons in 6 minutes. The current speed of this event reaches  $0.85 \text{ ms}^{-1}$ . The travel time from oil platform to FSO is about 1 hour and propagation speed relatively equal to  $1.12 \text{ ms}^{-1}$ , this time was evaluated through the distance (4033 m) between oil platform and FSO;
3. The soliton packets were identified with between 3 and 8 individual solitons. They propagate towards North-North-West with mean current speed of  $0.35 \text{ ms}^{-1}$  and mean propagation speed of  $0.6 \text{ ms}^{-1}$  during the study time;
4. The occurrence of an extreme squall event on 6 June 2014 at 17:40 UTC on FSO (figure 5.9 ), where the wind speed increased from 11 to  $23 \text{ ms}^{-1}$  in 24 minutes and wind direction changed from 210 to 100 °T. The FSO heading deviated from 195 to 130 °T. The FSO have displaced due to the absence of correlation between the heading deviation and curvilinear displacement;
5. The squall events were recorded with main wind speed of  $11.5 \text{ ms}^{-1}$  with a likely propagation direction from South-West, with a mean rise time of about 14 minutes;
6. Beyond the soliton event which led to the breaking of the mooring hawser, a violent response of tandem and FSO to soliton events was noticed, with a mooring hawser tension of up to 235 tons on 24 April 2014 at 06:35 UTC. The FSO heading deviation from 320 to 270 °T were observed.
7. The response of the mooring hawser and FSO was observed throughout the duration of the passage of the soliton on FSO, whereas the response of FSO to the squall event was only during the rise time of wind speed.

## 5.2 Recommendations

- Solitons and squalls are dangerous phenomena for offshore offloading operations, so it is necessary to obtain all the parameters which allow to predict efficiently the arrival of solitons and squall events during offshore drilling and offloading. Prediction of these events contributes to improving the cost effectiveness and will also the company to avoid any incident.
- It is necessary to know temperature and conductivity of all water column for soliton event, air temperature, air pressure, humidity and rainfall for squall event. In view of the low correlation between the semi-diurnal tidal cycle and the soliton occurrence in this area, it is indispensable to deepen the study of soliton propagation in the Gulf of Guinea, with SAR imagery which will enable the location of the generation site and to follow the trace of the soliton. It would also be beneficial to evaluate the influence of the Niger river discharge, dynamics of surface and sub-surface currents and ITCZ position on solitons.
- It would be important to use the different wind data around this area (if it exist) to find the time that will hold FSO personnel to position FSO (bow or stern) and Shuttle tanker towards the coming wind direction or to take any safety action.
- The mean travel time of solitons from oil platform to FSO is 1 hour 45 minutes, but a strong soliton can reach the FSO in less than 1 hour. It is therefore important for this oil company to install a soliton early warning system desk in real time on FSO.
- It would be yet extremely important to do a time-domain simulation of FSO-tanker response in a tandem offloading operation, knowing the current, wave and current characteristics, hawser diameter and wet weight, FSO and tanker length, breath, depth and displacement. The minimum relative distance, maximum relative heading and maximum hawser tension of offloading systems could be obtained. Thus, we optimize the parameters of the system and extend operating limits.

# Bibliography

---

- [1] Alvarez, J., P. Orsero, V. Quiniou-Ramus, M. François, A. G. Moysan, D. l'Hortis, and A. Ledoux (2011, January). Squall Response Based Design of Floating Units in West Africa, *In ASME 2011 30th International Conference on Ocean, Offshore and Arctic Engineering*, American Society of Mechanical Engineers, 233-242.
- [2] Apel, J. R., J. R. Proni, H. M. Bryne, and R. L. Sellers (1975). Near-Simultaneous Observations of Intermittent Internal Waves on the Continental Shelf from Ship and Aircraft, *Geophys. Res. Lett.*, 2, 4, 128-131.
- [3] Apel, J. R.(1987). Principle of Ocean Physics, Academic Press, 38, 634pp.
- [4] Apel, J. R., and D. M. Franer (2000). Nonlinear Solitary Internal Waves, *Global Ocean Associates (GOA)*, 2000-2, 16pp.
- [5] Apel, J. R., L. A. Ostrovsky, Y. A. Stepanyants, and J. F. Lynch (2006). *Internal Solitons in Ocean*, Woods Hole Oceanographic Institution, 110pp.
- [6] Berkes, F., P. Knippertz, D. J. Parker, G. Jeans, and V. Quiniou-Ramus (2012). Convective Squall over the Eastern Equatorial Atlantic. *Wea. Forecasting*, 27,770-783.
- [7] Bourles, B. (2008). Introduction to the Physical Oceanography Course, ICMPA-UNESCO Chair, Version 2, 193pp.
- [8] Bjerknes, J. (1919). On the Structure of Moving Cyclone, *Geofys. Publ.*, 1, 1-8.
- [9] Brugts, H., and M. Krekel (2004). FPSO Operations on DP, *In FPSO Research Forum* 58pp.
- [10] Chen, H. and T. Moan (2003).Probabilistic Modeling and Evaluation of Collision between Shuttle Tanker and FPSO in Tandem Offloading, Reliability Engineering and System Safety, 84, 169-186.
- [11] Clarke, A. J., and D. S. Battisti (1983). Identification of the Fortnightly Wave Observed Along the Northern Coast of the Gulf of Guinea, *J. Phys Oceanogr.*, 13, 2192-2200.
- [12] Dublin-Green, C.O., L.F. Awosika, and R. Folorunsho, (1999). Climate Variability Research Activities in Nigeria. National Statements: Nigeria *Nigerian Institute for Oceanography and Marine Research, Lagos, Nigeria*.
- [13] Duggal, A. S., and S. Ryu (2005). The Dynamics of Deepwater Offloading Buoys. *Fluid Structure Interactions and Moving Boundary Problems*, 269-278.

- [14] Fraser, N. (1999). Surfing and Oil Rig, *Energy Review*, 20-24.
- [15] Fraser, N. (1998). Natural Phenomena abound in the Bay of Bengal, *Professional Mariner*, 30, 20-21.
- [16] Fugro GEOS (2004). *West African Gust Joint Industry Project. Phase 1 Final Report*, 1, C56110/3219. Confidential.
- [17] Fugro GEOS (2010). *Odudu Internal Wave Characterisation*, C70027/7585/R0. Confidential.
- [18] Goff, M., G. Jean, L. Harrington-Missin, and C. Baschenis (2010). Soliton Early System for Offshore, 2010, Applications, *In Oceanology International*, 12pp.
- [19] Hamilton, R.A. and J.W. Archbold (1945). Meteorology of Nigeria and adjacent territory, *Q. J. R. Meteorol. Soc.*, 71, 231-264.
- [20] Hyder, P., G. Jeans, E. Cauquil, R. Nerzic, R. Gao, and R. Stephens (1999). The characteristics and generation of internal solitons observed at a proposed drilling location offshore Myanmar, *Proc. Oceanology International*, 20pp.
- [21] Infeld, E., and G. Rowlands (2000). *Nonlinear Waves, Solitons and Chaos*, Cambridge University Press.
- [22] IOC/CEC (1993). *Manual of Quality Control Procedures for Validation of Oceanographic Data*
- [23] Jackson, B., S. E. Nicholson, and D. Klotter (2009). Mesoscale convective systems over western equatorial Africa and their relationship to large-scale circulation, *Mon. Wea. Rev.*, 137, 1272-1294.
- [24] Jeans, G. (1998). A Nonlinear Tide on the Portuguese Shelf, *Thesis Submitted to the University of Wales*.
- [25] Jimoh, Olayinka R. (2010). Internal Waves and Solitons Offshore Nigeria, *Master Thesis, ICMPA, University of Abomey-Calavi*, 45pp.
- [26] Legerstee, F., M. François, C. Morandini, and S. Le-Guenne (2006). Squall: Nightmare for Designers of Deepwater West African Mooring Systems, *In 25th International Conference on Offshore Mechanics and Arctic Engineering*, American Society of Mechanical Engineers, 171-176.
- [27] McPhail, Finlay (2014). The Effects of Squalls on FPSOs, *Shell Global Solutions B.V. Publication*, 47pp.
- [28] Ojinnaka, O. C. (2006). The Nigerian Vertical Datum and the Influence of the Degenerate Amphidrom, *The Proceedings of Nigerian association of Geodesy Conference*, Geodesy and National Development.
- [29] Osborne, A. R., and T. L. Burch (1980). Internal Solitons in the Andaman Sea, *Science*, 208, 4443, 451-460.

- [30] Ostrovsky, L., and Y. A. Stepanyants (1989). Do Internal Exist in The Ocean, *Rev of Geophysics*, 27, 293-310.
- [31] Parker Doug (2004). Review of Squall Characteristic in the Atlantic off the West Coast of Africa, Version 1.0, 18pp.
- [32] Ramp, S. (2006). *The Windy Islands Soliton Experiment*, Naval Postgraduate School brochure, Dept. of Oceanography.
- [33] Santala, M. J., M. Calverley, S. Taws, H. Grant, A. Watson, G. Jean (2014, May). Squall Wind Elevation/Gust Factor and Squall Coherence, In *Offshore Technology Conference*, Offshore Technology Conference USA, 7pp.
- [34] Shanmugam G.(2013). Modern Internal Waves and Internal Tides along Oceanic Pycnoclines: Challenges and Implications for Ancient Deep-marine Baroclinic Sands, *AAPG Bulletin*, 97(5), 767-811.
- [35] WMO (1962). Supplement to the WMO Publication No. 122.RP50 abridged final report of the third session of the Commission for Synoptic Meteorology, World Meteorological Organization, 228pp.
- [36] Yang, G. Y., and J. Slingo (2001). The diurnal Cycle in the Tropics. *Mon. Wea. Rev.*, 129, 784-801.
- [37] <http://www.aukevisser.nl/supertanker/FPSO-FSO/id555.htm>

---

# Appendix

---

*Appendix 1 : Some responses of FSO and shuttle tanker to soliton event*

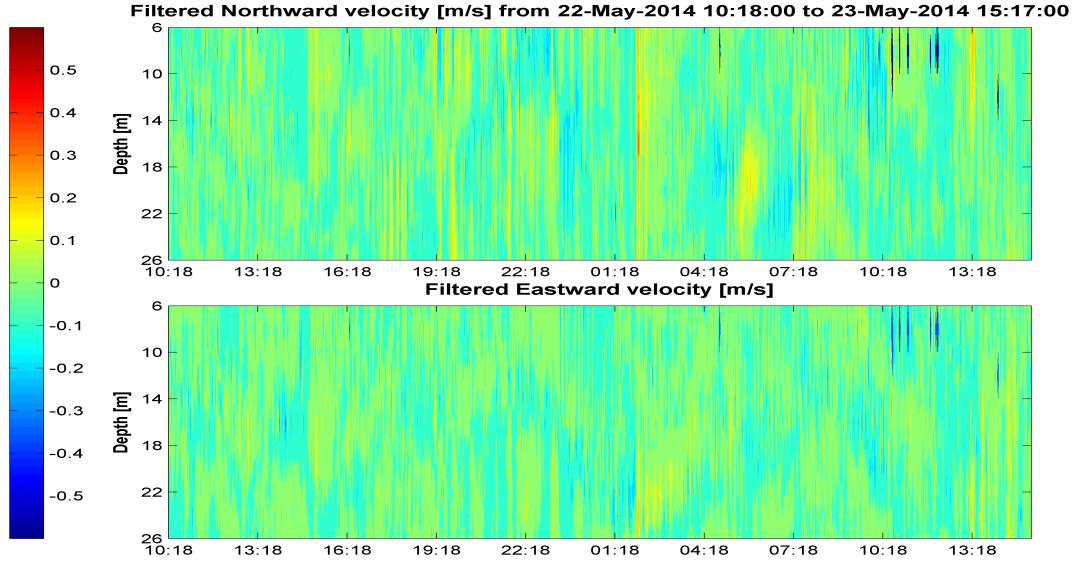


*Fig. 5.1: Contour plots of filtered Northward and Eastward velocity showing the arrival of soliton event at 01:40 on 23 May 2014 at platform.*

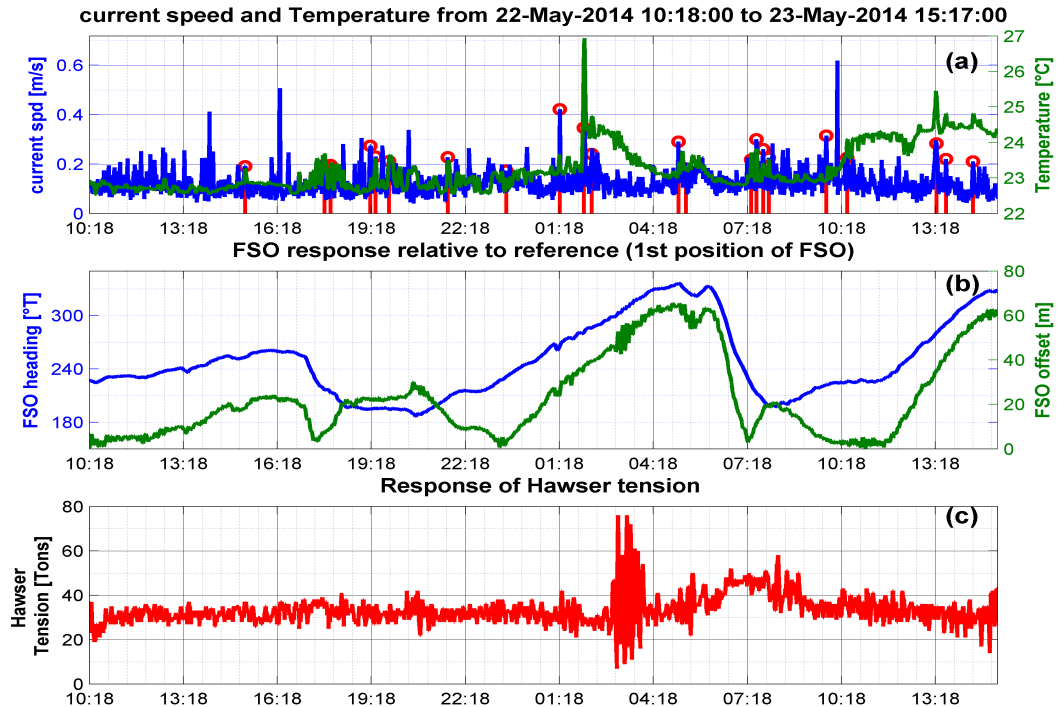


*Fig. 5.2: plots of current speed and temperature (a), FSO displacement and heading (b) and hawser tension (c) showing the response of FSO and mooring hawser to soliton event between 02:45 and 04:00 UTC on 23 May 2014. We can notice an inclination of heading from 240 to 320 °T and an increase of hawser tension up to 78 tons.*

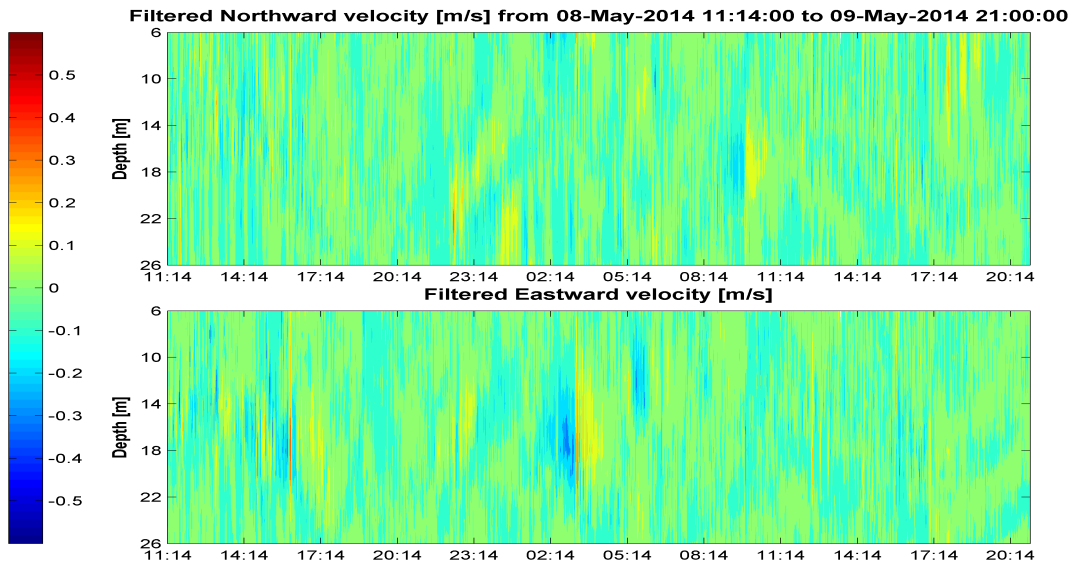


Fig. 5.3: Contour plots of filtered Northward and Eastward velocity showing the arrival of 3 soliton events at 16:40 on 8 May 2014, at 03:30 and 12:30 on 9 May 2014 at oil platform

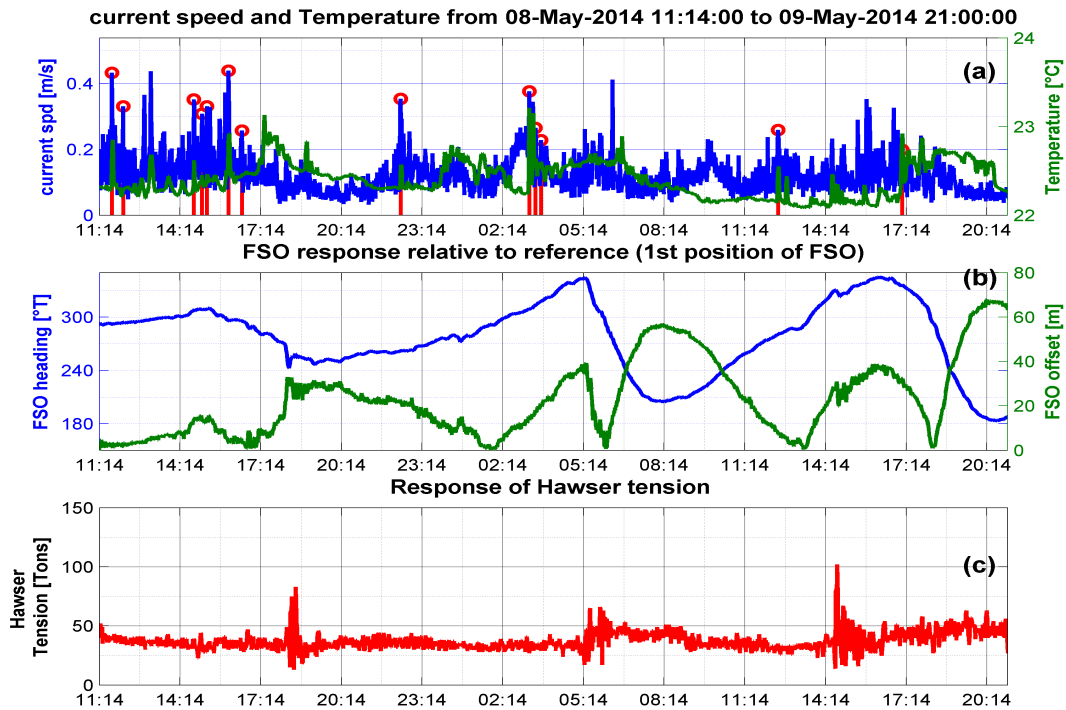


Fig. 5.4: plots of current speed and temperature (a), FSO displacement and heading (b) and hawser tension (c) showing 3 main responses of FSO and mooring hawser to soliton event. We can notice an inclination of heading from 240 to 320 °T and an increase of hawser tension up to 100 tons between 14:00 and 16:45 on 09 May.

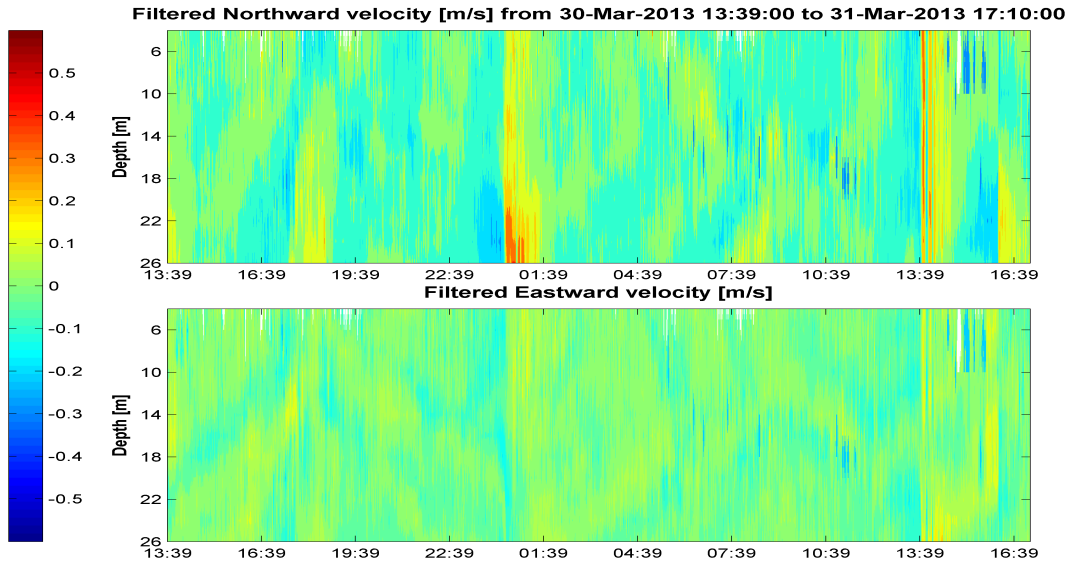


Fig. 5.5: Contour plots of filtered Northward and Eastward velocity showing the arrival of 2 soliton events at 00:00 and 13:30 on 31 March 2013 at oil platform .

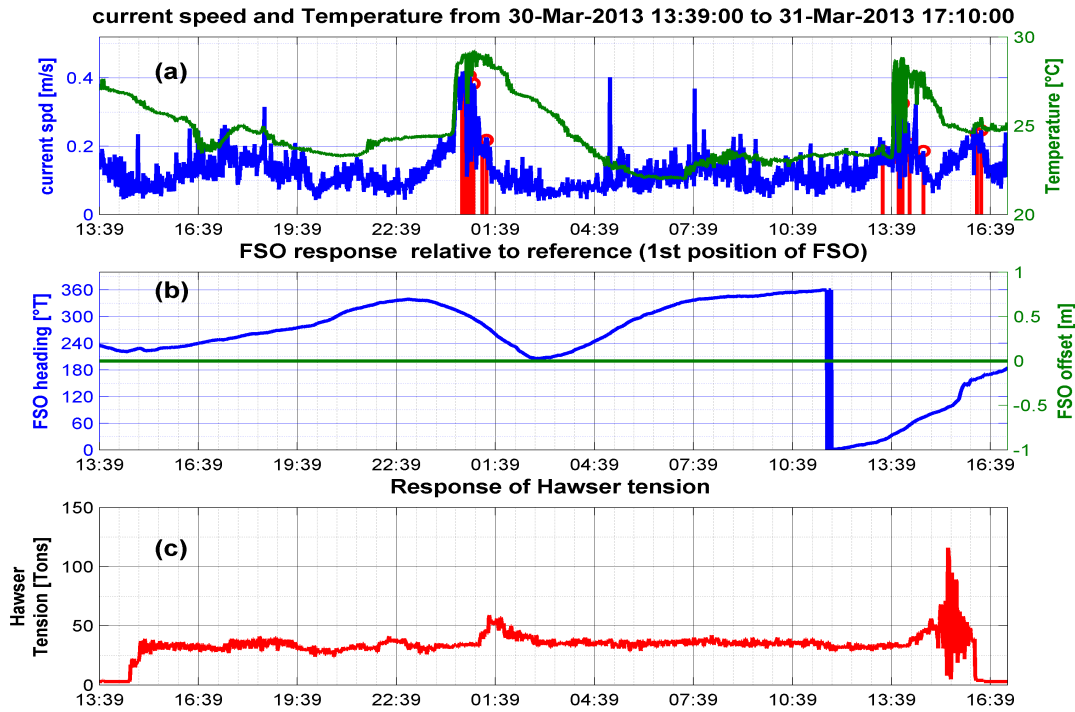


Fig. 5.6: plots of current speed and temperature (a), FSO heading (b) and hawser tension (c) showing 2 main responses of FSO and mooring hawser to soliton event. We can notice an inclination of heading from 300 to 200 °T from 00:45 to 02:10 on 31 March 2013 and an increase of hawser tension up to 120 tons between 14:30 and 15:45 on 31 March 2013.

## Appendix 2: Some FSO response cases to squall events

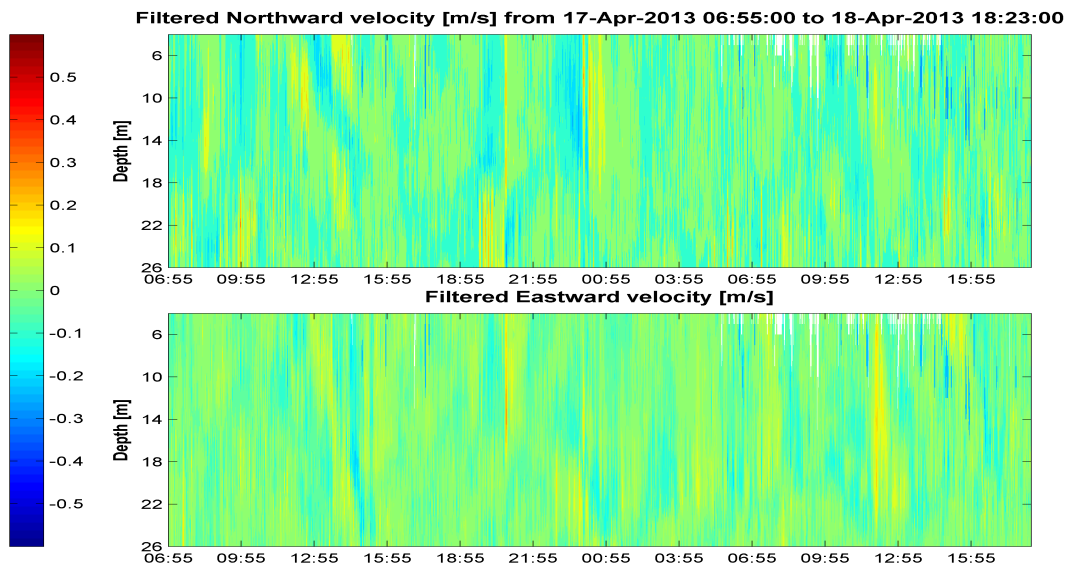


Fig. 5.7: Contour plots of filtered Northward and Eastward velocity showing the arrival of some soliton events at oil platform .

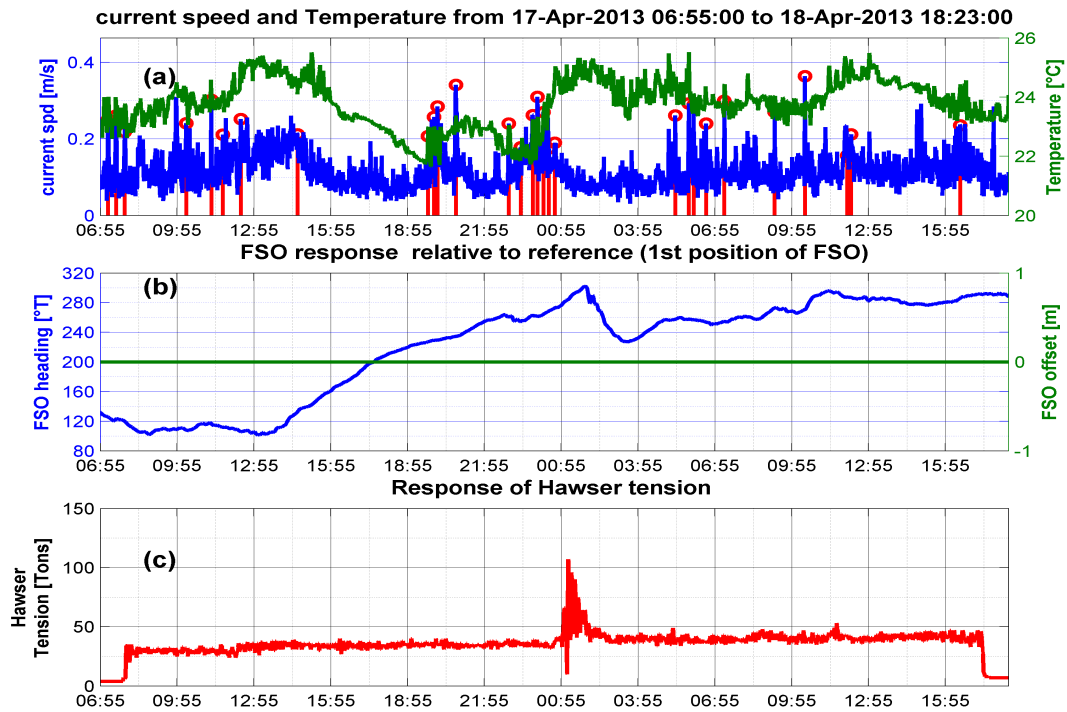


Fig. 5.8: plots of current speed and temperature (a), FSO heading (b) and hawser tension (c) showing FSO and mooring hawser response to soliton event. We can notice an inclination of heading from 240 to 300 °T and increase of hawser tension up to 105 tons between 01:00 and 02:30 on 18 April 2013.

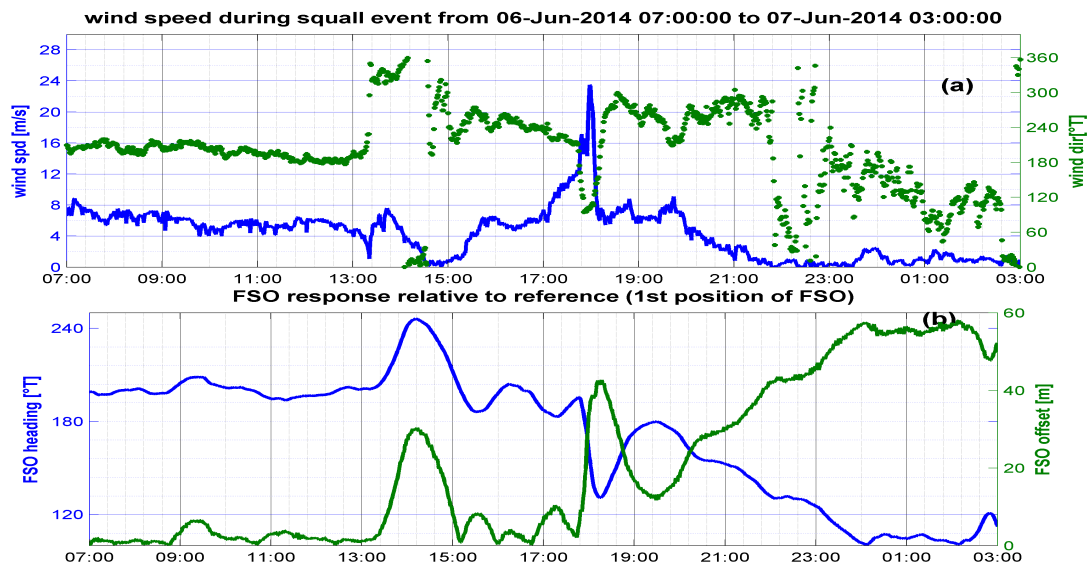


Fig. 5.9: 22-hour plots of wind speed and direction (a), FSO displacement and heading (b), showing the response of FSO to arrival of squall event at 17:00. We can notice heading change from 195 to 130 °T and horizontal displacement of FSO.

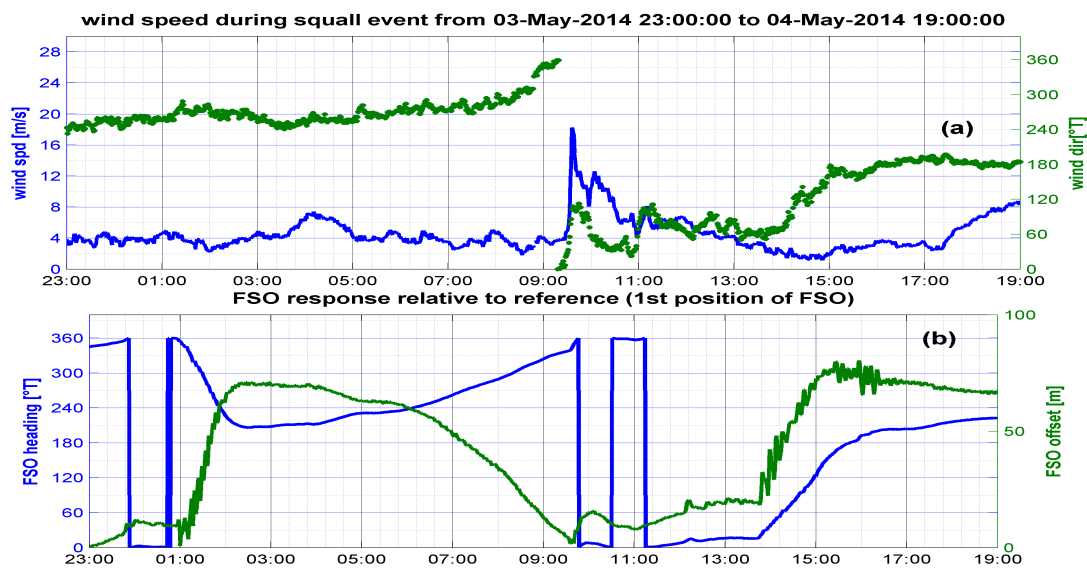


Fig. 5.10: 22-hour plots of wind speed and direction (a), FSO displacement and heading (b), showing the response of FSO to arrival of squall event at 09:30. We can notice heading change from 300 to 10 °T.